HBV

HØGSKOLEN I BUSKERUD OG VESTFOLD · PROFESJONSHØGSKOLEN ·

FACULTY OF TECHNOLOGY
AND MARITIME SCIENCES

Micro and Nano Technologies for Unmanned Nano Air Vehicles (NAVs)

Doctoral Thesis

Luca Petricca

2014

FACULTY OF TECHNOLOGY AND MARITIME SCIENCES

Micro and Nano Technologies for Unmanned Nano Air Vehicles (NAVs)

Thesis submitted for the degree of Philosophiae Doctor

Luca Petricca

Department of Micro- and Nanosystem Technology (IMST)
Faculty of Technology and Maritime Sciences (TekMar)
Buskerud and Vestfold University College (HBV)
Horten, 2014

Micro and Nano Technologies for Unmanned Nano Air Vehicles (NAVs)

Department of Micro- and Nanosystem Technology (IMST)
Faculty of Technology and Maritime Sciences (TekMar)
Buskerud and Vestfold University College (HBV)
Horten, 2014

Doctoral theses at Buskerud and Vestfold University College, no. 2

ISSN: 1894-6380 (print)
ISBN: 978-82-7860-243-0 (print)
ISBN: 978-82-7860-242-3 (online)

Cover: HBV, Kommunikasjonsseksjonen

Preface

This Ph.D. project was part of the collaboration between Høgskolen i Vestfold and Prox Dynamics AS, supported by the Research Council of Norway through the "Mosquito project" (NRF/BIA number 193252/I40). It was focused to find micro and nano technologies for Nano Unmanned Aerial Vehicles (UAV). Professor Per Ohlckers has been my main supervisors while Professor Knut E. Aasmundtveit and Trygve F. Marton were my co-supervisors during my Ph.D. studies. The work presented here was mainly carried out in the MST labs at Høgskolen i Vestfold (Norway) and in the aerospace engineering department of University of Maryland (UMD), in USA. This thesis is based on five published papers and one submitted for publication in scientific journals (Appendix) In addition, several papers were presented at international conferences.

A special thanks to my supervisor Per Ohlckers for guiding me during these four years. I would express also my gratitude to my co-supervisors for their advices and feedbacks. Also, many thanks to all the people at IMST who helped me during these years, in particular Ragnar Dahl Johansen for his assistance in the labs and Nils Høivik and Tone Gran for their help with administrative issues. Additional thanks to all the other researchers and co-authors of my papers, which have collaborated with me in many direct and indirect ways.

Thanks to Prof. Inderjit Chopra from University of Maryland, for hosting my research period at UMD and to Dr. Vikram Hrishikeshavan for his cooperation on developing the ELKA board.

Thanks also to my wife Elka (yes, like the board!) for her encouragements and to my family for their support and assistance.

I also would like to express my gratitude to all the other people not explicit mentioned here but that helped me to reach this important milestone.

Thank you again to all of you!

Oslo November 2013,

Luca Petricca

Abstract

Nano Air Vehicles (NAVs) consist of remotely controlled miniaturized flying objects with maximum dimensions smaller than 15 cm and less than 20 g in weight. The small size of such systems allows them to penetrate and collect data from regions that are inaccessible to other vehicles. They could provide great advantage in many life threatening situations. Intelligence Surveillance and Reconnaissance (ISR) are typical applications for NAVs. They can also be used as extended senses in dangerous environments such as collapsed mines and buildings; disasters in nuclear power plant etc.

Despite their small size, these vehicles are extremely complex and provide a fusion of different research areas such as micro technology, electronics, material science, informatics, control theory, mechanics, aerodynamics and physics. Many large universities and institutes (such as [1] (DARPA)) have been studying and developing them for almost ten years.

This Ph.D. work is focused on finding micro and nano technologies suitable to be used onboard in NAVs. It starts with the review of the state of art of such systems, breaking them into basic blocks and finding the integration bottlenecks. We then investigated micro technologies based devices that can be used to improve their performance. In particular, we present piezoresistive accelerometers and microphones fabricated with the MultiMEMS process, with an explanation of the measurement set up used and the results from the analytical and Finite Elements Method (FEM) models of the sensors.

The work continues presenting a simple and innovative solution for PCB to PCB interconnections. It consists of a small interposer complete with multiple vias to be placed in between two PCB boards. The interposer is designed for creating electrical and mechanical connections at the same time, while leaving enough space in between on the PCBs for electric component placement. The reliability of this solution has been tested by vibration and temperature cycling tests.

During this project, it also developed one of the smallest autopilot system in the world based on STM32 microcontroller and complete with 2.4 GHz wireless interface and 9 axis

DOF inertial motion unit (IMU). The small dimensions (28x21 mm^2) and the low weight (1.2 g) of this autopilot, makes it the perfect candidate to be used onboard in NAVs.

The thesis includes also a review of energy storage systems, their limitations and possible alternatives, for future vehicles. Furthermore, I also present the initial work done on supercapacitor devices based on black silicon, including the fabrication and analysis of two different silicon wafers as well as a suggested detailed process for the creation of those devices.

Table of contents

PREFACE ..... **III**

ABSTRACT ..... **V**

TABLE OF CONTENTS ..... **VII**

LIST OF PAPERS: ..... **IX**

LIST OF ABBREVIATION ..... **XI**

1 INTRODUCTION **1**

1.1 Research Goal and Approach 3

1.2 Structure of the Thesis 5

2 SENSORS **7**

2.1 The MultiMEMS Process and the Piezoresistive Principle 7

2.2 Accelerometers 9

2.3 Microphones 12

3 INTERCONNECTIONS **17**

3.1 Cables and Connectors 17

3.2 Interposer Technology 18

3.2.1 Interposer Tests and Results 21

4 THE AUTOPILOT **23**

4.1 ELKA Design and Fabrication 24

4.2 ELKA Tests 28

5 ENERGY STORAGES 33

5.1 Black Silicon Supercapacitor.....34

6 CONCLUDING REMARKS AND FUTURE PROSPECTIVE..... 39

BIBLIOGRAPHY 41

***APPENDIX* 45**

List of Papers:

Journal Papers:

1 Luca Petricca, Ohlckers, Per and Grinde, Christopher: "*Micro- and Nano-Air Vehicles: State of the Art*" International Journal of Aerospace Engineering. Volume 2011, Article ID 214549, 17 pages. DOI:10.1155/2011/214549

2 Luca Petricca, Christopher Grinde and Per Ohlckers: "*A miniaturized bulk micromachined triaxial accelerometer fabricated using deep reactive etching through a multilevel thickness membrane*" Journal of Microsystem Technologies, Springer, Volume 18, Number 5 (2012), 613-622, DOI: 10.1007/s00542-012-1429-9

3 Luca Petricca; Per Ohlckers; "*Analytic model and FEM characterization of two piezoresistive microphone membrane.*" MEMSM 2013: Proceedings of the MEMS Mechanics, 15-16 March 2013, Wuhan, China and published on Advanced Materials Research (ISSN: 1022-6680).

4 Luca Petricca, Per Ohlckers and Geir Mortem Mellem; "*Ultra low weight spacer for PCB2PCB interconnections.*" Published in IMAPS Journal of Microelectronics and Electronic Packaging issue 1 2014 (ISSN 1551-4897).

5 Luca Petricca, Vikram Hrishikeshavan, Per Ohlckers and Inderjit Chopra *"Design, fabrication and test of an Embedded Lightweight Kinematic autopilot (ELKA)"* Accepted for publication to International Journal of Intelligent Unmanned Systems, ISSN: 2049-6427

6 Luca Petricca, Per Ohlckers and Xuyuan Chen (2013). *"The Future of Energy Storage Systems",* Book chapter form: Energy Storage - Technologies and Applications , ISBN: 978-953-51-0951-8, InTech, DOI: 10.5772/52413. Available from: http://www.intechopen.com/books/energy-storage-technologies-and-applications/the-future-of-energy-storage-systems

Conference Papers:

7 Per Ohlckers, Luca Petricca, Christopher Grinde; "A Silicon Micromachined Triaxial Accelerometer Using the MultiMEMS MPW Process with Additional Deep Reactive Ion Etching as Post-processing" Proceedings of the 21st MME2010 (MicroMechanics Europe), Twente, the Netherlands, September 26-28, 2010, ISBN 978-9081673716.

8 Luca Petricca, Ohlckers, Per and Grinde, Christopher: "*A Review of Nano Air Vehicles*" Proceedings of COMS2010 (Commercialization of Micro-Nano Systems)**,** Albuquerque, New Mexico, August 29 – September 2, 2010.

9 Luca Petricca; Grinde, Christopher; Lowrie, Craig; Ohlckers, Per; "*Triaxial accelerometer fabricated using the MultiMEMS process with a deep reactive etching as additional step.*" MME 2011: Proceedings of the 22nd Micromechanics and Microsystems Europe; 19-22 June 2011 Tønsberg, Norway. ISBN 978-82-7860-224-9. s. 314-317

10 Luca Petricca, Per Ohlckers, Xuyuan Chen: "*Review: The future of energy storage systems using micro- and nanotechnologies*" Proceedings of the 18th World MicroMachine Summit 2012**,** Hsinchu, Taiwan, April 23 – 26, 2012.

11 Luca Petricca; Ohlckers Per; Wang Dag; "*COMSOL models of two different microphones membrane with a piezoresistive sensing element.*" MME 2012: Proceedings of the 23rd Micromechanics and Microsystems Europe workshop: 9-12 September 2012 Ilmenau, Germany.

12 Luca Petricca; Ohlckers Per, Geir Mortem Mellem "*Ultra Low Weigh Solution for PCB Interconnections*" MME 2013: Proceedings of the MME, 1-4 September 2013, Espoo, Finland.

The work has also been presented at the following workshops:

13 Luca Petricca: "*Optimization of nano unmanned aerial vehicles*", Invited speaker at Norwegian Ph.D. Network on Nanotechnology for Microsystems, Tønsberg, Norway, 31. May- 2. June 2010

14 Luca Petricca "*Triaxial accelerometer fabricated using the MultiMEMS process with a deep reactive etching as additional step*" The Norwegian Ph.D. Network on Nanotechnology for Microsystems, Oslo, Norway, 15-17 June 2011

15 Luca Petricca: "*A review on energy storage systems*", Invited speaker at Norwegian Ph.D. Network on Nanotechnology for Microsystems, Trondheim, Norway, 11-13 June 2012

16 Luca Petricca, Per Ohlckers and Geir Morten Mellem "*Ultra low weight spacer for PCB2PCB interconnections"* Petricca Luca, Per Ohlckers and Geir Morten Mellem. The Norwegian Ph.D. Network on Nanotechnology for Microsystems, Bergen, Norway, 17-19 June 2013

Other papers from the author:

17 Luca Petricca; Aasmundtveit, Knut E.; Nguyen, Hoang Vu; Hoivik, Nils. "*Au Stud Bump Optimization for Anisotropic Conductive Adhesives Film Interconnects.*" IMAPS Nordic 2010 Conference; 2010-06-06 - 2010-06-09

List of Abbreviation

ALD	Atomic Layer Deposition
DAQ	Digital Acquisition Board
DARPA	Defense Advanced Research Projects Agency
DOF	Degree of Freedom
DSP	Double Side Polished (silicon wafer)
EDCL	Electric Double Layer Capacitors
ELKA	Embedded Lightest Kinematic Autopilot
EPC	Electrochemical Pseudo Capacitors
FEM	Finite Elements Methods
FFC	Flexible Flat Cable
FR4	Flame Retardant (Material)
GBS	Ground Base Station
GINA	Guidance and Inertial Navigation Assistant
GPIO	General Purpose Input Output pin
GPS	Global Position System
IMU	Inertial Motion Unit
ISR	Intelligence, Surveillance, Reconnaissance
LCD	Liquid Crystal Display
MAV	Micro Air Vehicles
NAV	Nano Air Vehicles
PCB	Printed Circuit Boards
PWM	Pulse Width Modulation
SSP	Single Side Polished (silicon wafer)
TPM	Tire Pressure Monitoring

1 Introduction

Nano UAVs are natural evolution of larger vehicles called Micro Air Vehicles (MAV). Their official birth is in general associated with the year 2005, when DARPA launched the first official research program [3]. The project was focused on developing small flying objects with maximum dimension of 15 cm and less than 20 g in weight [4]. Thanks to the potential large market and numerous application areas of such systems, many other companies and institutes got interested to develop such technology. Nano Air Vehicles (NAV) are the perfect candidates to be used in all those environments where humans cannot reach, because of their great capability of exploring dangerous areas that are inaccessible to other media. The most interesting application of these vehicles is as surveillance drones, for tracking chemical, biological or radioactive threads. As correctly predicted in the ARTICLE I (See Article Section), they are now already in the market and actively used by soldiers in the battlefields. British Army and U.S. Army are now officially adopting such technology. As reported by many media [5] [6], they used these vehicles in many harsh combat regions such as Afghanistan. In this context, these miniaturized drones are used by personnel to observe dangerous areas from a secure cover. Once that they ensure that the perimeter is clear, soldiers can move into the area safely, thus reducing casualties and wounded. Current systems (such as the one adopted by British and U.S. Army), have onboard GPS, three cameras, accelerometers and gyroscopes [7]; however, it is reasonable to think that in the near future those system will include more sensors such as microphones, temperature sensors, several chemical sensors, night camera, etc. Many of these sensors will only be required on some specific missions, such as the investigation of suspect buildings for finding hazardous materials.

This military use is not the only application for the technology. Civilian police forces and firefighters could use NAVs to search for survivors in case of fire in buildings, collapsed mines and nuclear power plant disasters. Furthermore in case of chemical accidents they

can be used for tracking toxic gases, monitoring for example the extension and the concentrations of the toxic gas cloud. With so many stakeholders involved, numerous universities, companies and foundations have started to investigate the possibility to create small flying objects. Basically, all the solutions found can be categorized into four classes. The first class consists of fixed wings vehicles. This class is a small version of a large aircraft. Unfortunately they are not able to hover and thus they are less suitable for indoor flying.

The second class consists of rotary wings vehicles. In reality this class contains many different solutions based on the numbers and the position of the propellers, each one with its own advantages and drawbacks. Some of these designs are reported in Figure 1.

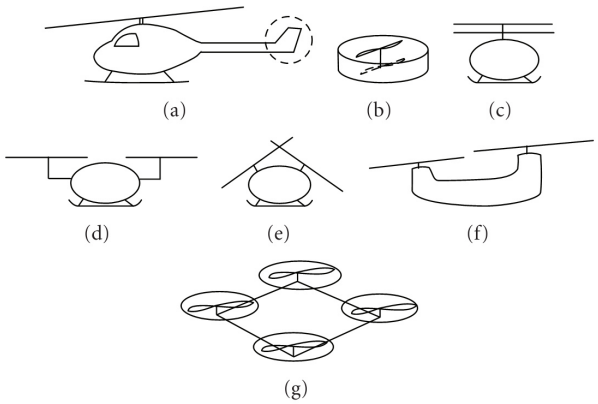

Figure 1. Graphic representation of rotary-wing configurations: (a) conventional configuration, (b) ducted coaxial, (c) conventional coaxial, (d) rotors side by side, (e) synchropter, (f) conventional tandem, (g) quad rotor.

Most of the commercially available NAVs such as the "Black Hornet 100" from "Prox Dynamics" [7] or the "Crazyflies" from "Bitcraze" [8] can be placed in this category.

The third category is inspired by nature and consist of flapping wings vehicles. Those systems can be very small and efficient, especially at reduced scales. A good example is represented by the "micro-robotic bee" prototype recently developed at Harvard. "RoboBee" (official name) weighs less than 100 mg and is able to lift its own weight [9]. However, this small vehicle was powered by cables and it does not include any battery because of the difficulties to have a light and efficient energy storage system onboard [10]. Despite still being research based technology, this category has undergone great progress in the last years, mainly initiated by the introduction of piezoelectric motion solution. Particularly interesting are also hybrid bio-solutions. Similar to sci-fi movies, these cyborgs are structures where insects and electronics are merged together [11] in order to create a

perfectly controllable system. Working examples of such futuristic solution are provided from Berkeley University. In particular there were able to implant probes into the beetle's brain and muscles (they were implanted at the larva stage) and controlling them by applying small electrical signals [12]. The limitation of such a system is the low payload that the insect can transport, reducing the practical use in real missions.

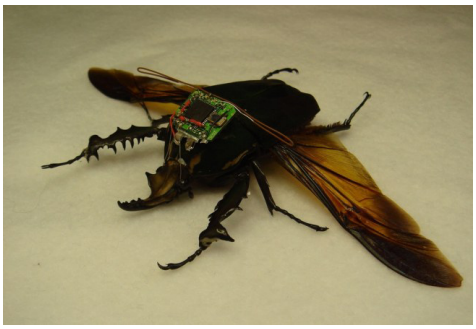

Figure 2. Beetle hybrid system: university of Berkeley **[13]**.

The last category is represented by passive vehicles. These systems such as gliders or blimps have no thrust and must be hand-launched or dropped from other aircrafts and thus their application is probably limited to climate control (winds direction) or similar areas. This last category is very different in concept and do not include any active control. They will not be considered in this work.

1.1 Research Goal and Approach

As already discussed in the previous paragraph, NAVs can play an important role in both surveillance and defense applications. Despite their small size, they are extremely complex systems, with limited weight, space and power budgets. Some components used onboard such as microcontrollers, capacitors, resistors etc., have been in the market in reduced dimensions for many years. Others such as Inertial Motion Units (IMU), cameras and GPS have only recently become available in the market, mainly thanks to the push of smartphone technology. In this thesis we explored possible micro and nano technologies that can help to reduce weight and size of the current vehicles or alternatively to increase the functionalities keeping the size constant (integration).

Despite the seemingly very different working concepts of the three active vehicle categories explained in the previous paragraph, they would look more similar if we considered the

block diagram of those classes and compared them. Indeed most of the vehicle parts are generic and thus are more or less independent from the final configuration. In Figure 3 the main blocks of a NAV are shown. Blocks such as Power management, Sensors, Communication and Processors are the same in all the vehicles. The only block that has some dissimilarity is the Airframe, which includes the aerodynamics shape (different in each vehicle).

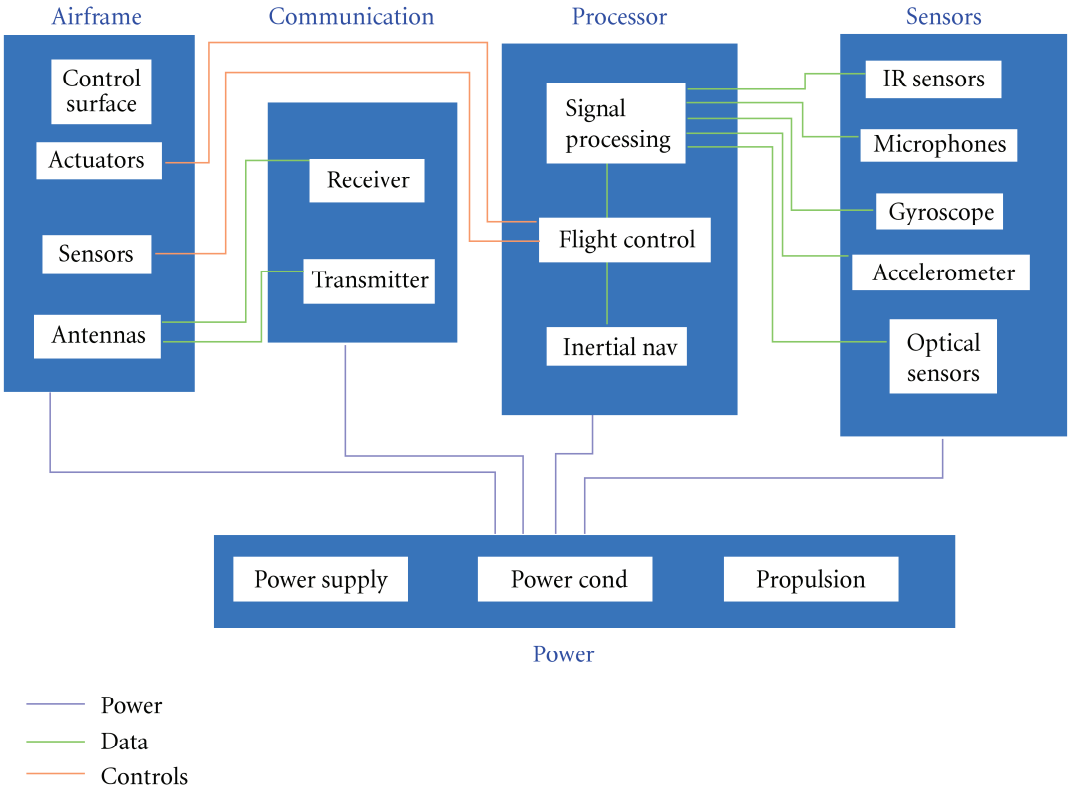

Figure 3. Block diagram of a nano air vehicle.

By using this level of abstraction, we can optimize most of the blocks, while being independent from the final vehicle design. In this work we used this approach, focusing mainly on the electronics and sensor parts with some additional work done on energy storage.

1.2 Structure of the Thesis

This work is organized in six chapters, including this introductory part (Chapter 1).

Chapter 2 reports the work done on sensors and the results of the measurements. The work has been performed on accelerometers and microphones fabricated by using the MultiMEMS process at Sensonor.

In chapter 3 a new technology for PCB to PCB interconnection is presented. It mainly consists of an interposer to be placed in between two boards which is able to create electrical and mechanical connection at the same time.

Chapter 4 presents the work done in the electronic part of the vehicles. In particular, it reports an overview of the Embedded Lightweight Kinematic Autopilot (ELKA). This circuit is one of the smallest autopilot systems in the world and it includes a 32-bit microcontroller, a 9 axis inertial motion unit (IMU) and a 2.4 GHz RF interface.

Chapter 5 presents some possible solutions for solving the energy storage problem onboard, with some ideas and initial work done for creating supercapacitors starting from black silicon wafers.

Conclusion and some discussions are available in the last chapter of this work.

2 Sensors

Sensors are vital elements present onboard in aerial vehicles. Based on the use of their data, they can be divided into two classes. The first class of sensors, such as accelerometers, gyroscopes, barometric sensors, magnetometers, GPS, etc., are used for flight and navigation functions. Without them, NAV would not be able to calculate its own position in space. The final purpose is to help the pilot navigate, stabilize the vehicle and gather flight data. The second class of sensors is not strictly required onboard and they are used for collecting data for missions. They are part of the payload and they can be customized suiting the application requirements. Gas sensors, radiation sensors, video cameras, microphones, night cameras etc. are part of this class.

In this chapter we have investigated the possibility to use piezoresistive sensors for both navigation (accelerometers) and payload purposes (microphones). The sensors we investigated were fabricated for other scopes, by using SensoNor MultiMEMS process available at the time as Multi Project Wafer (MPW). However we found the piezoresistive principle interesting; the high power consumption problem can be solved by duty cycling making the average power consumption very low. We wanted to further characterize this type of MEMS device for evaluating the possibility to create similar sensors suitable to be used onboard.

2.1 The MultiMEMS Process and the Piezoresistive Principle

MultiMEMS is the brand name of the MPW service that was offered by Sensonor to universities, research institutes and small companies [16]. It consists of a triple stack on glass-silicon-glass and it allows a precise electrochemical etch stop of membranes and masses of 3 and 23 µm in thicknesses. It also gives the possibility to use a 6 µm deep RIE

process in order to release thin membranes or create recesses in the device. The motion detection is done by using two types of piezoresistors: Surface resistors for thin membrane deflection detection and buried resistors (under the epitaxial layer) for thicker beams. Further features include the possibility to use buried conductors for crossing the anodic bonding area while keeping the cavities hermetic.

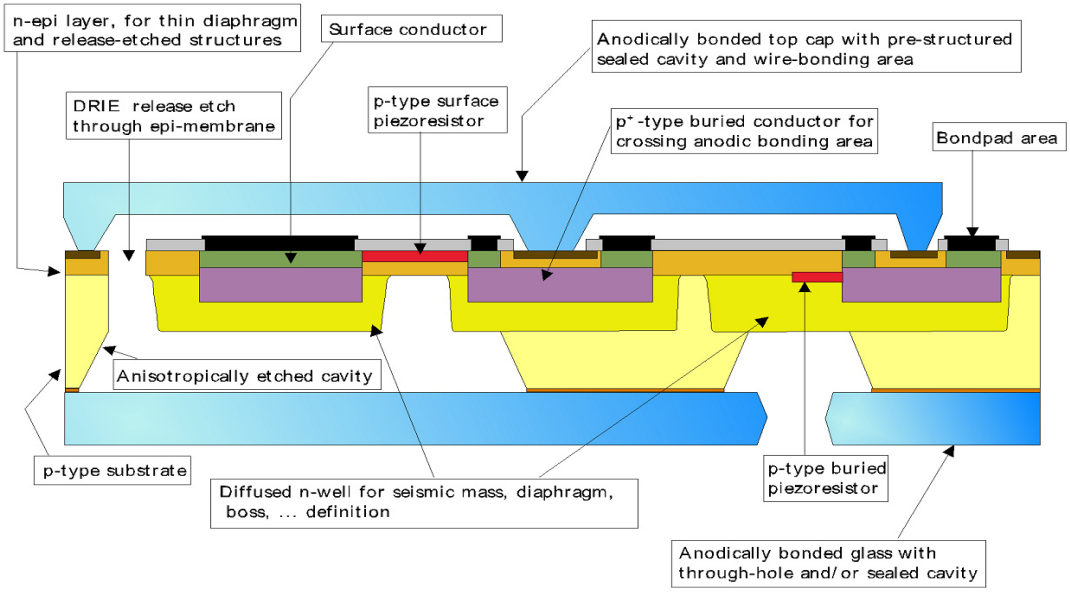

Figure 4. The MultiMEMS process: cross section view **[17]**.

The sensing elements for this technology (piezoresistors) are based on the piezoresistive effect, which is the change of the electrical resistivity with stress. The main equation that describes this effect is:

$$R = R_0(1 + \prod_L \sigma_L + \prod_t \sigma_t) \qquad \{1\}$$

Where R_0 is the stress free resistance value, σ_L and σ_t represent the stress levels in the resistor longitudinal and transversal directions while $\prod_L$ and $\prod_t$ are the piezoresistor coefficients for the longitudinal and the transversal directions respect the current direction in the resistor. Even though it could be enough to use a single resistor for detecting the membrane/mass motion (stress on the beam), this is in practice almost never done. A more common configuration is the Wheatstone bridge. It consists of a bridge of four resistors, where a fixed voltage is applied in two opposite corners while the reading is made between the other two. The main advantage of this method is the reduction of the thermal drift error

of the resistors. Moreover, by optimizing the resistor orientation in the design phase, it is possible to increase the sensitivity of the device and maximizing the output reading voltage. This technique has been successfully applied in many SensoNor devices used in many different fields such as the SA20 crash sensor [18] or the pressure sensors from family SPxx and the wafer family SW41x [19]. Some of these applications, such as the Tire Pressure Monitoring (TPM) sensor, require very low power consumption. Others such as aerospace, requires great reliability and accuracy. The wide application field of these devices has pushed us to investigate possible applications of piezoresistive sensors onboard the NAV.

2.2 Accelerometers

The 3-D accelerometers tested here were fabricated for biomedical application. Indeed, it has been demonstrated that accelerometer attached to the epicardium (the outer layer of the heart) can be used for early detection of heart ischemia [20] [21] [22]. Ischemia is mainly a postoperative problem in the first few days after a bypass heart surgery operation. It is therefore desirable to remove the accelerometer along with the pacemaker/EKG electrodes after this initial critical phase, pulling it out of the patient chest without any extra surgery.The device consists of two dual axis accelerometers rotated 90º to each other as shown in Figure 5.

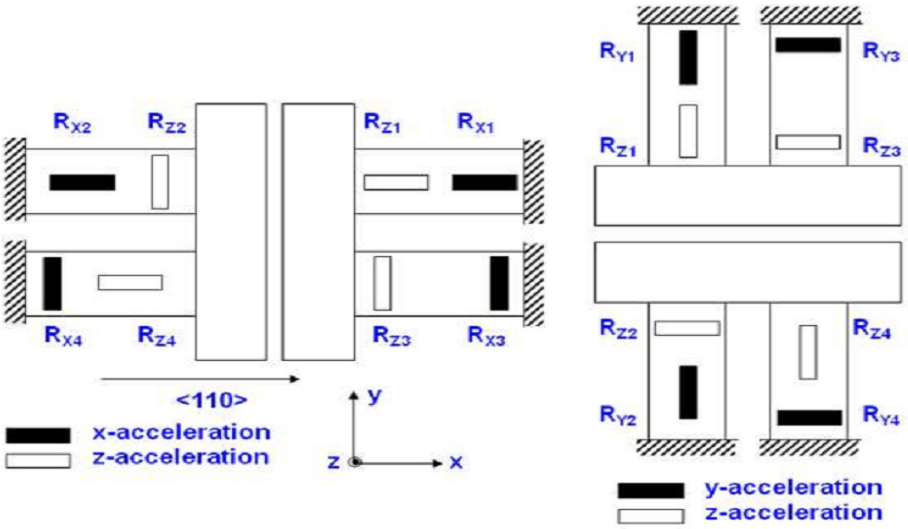

Figure 5. Overview of the 3D accelerometer.

Each section of the accelerometer consists of two masses attached to the frame by a thin beams. The beams are 23 µm in thickness, while the masses are 400 µm thick. The sensing elements consist on four piezoresistors implanted at the base of each beam. The piezoresistors are organized in a full Wheatstone bridge configuration, aligned such that each bridge provides acceleration data for one axis. Each 2-D structure is able to sense the acceleration coming from 2 axis; x-z or y-z. In case of the out of plane acceleration, the deflections of the two masses are in the same direction, while in case of in plane acceleration, the two masses are deflected in opposite directions, as shown in Figure 6.

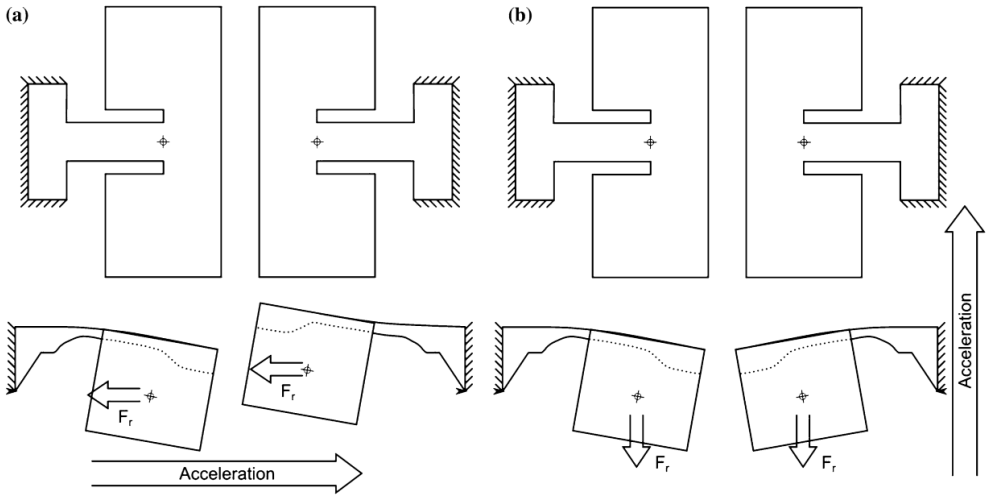

Figure 6. Mass deflection for in-plane acceleration (a) and out of-plane acceleration (b).

The devices (Figure 7) were fabricated using the MultiMEMS process explained in the previous paragraph with an additional DRIE process made at SINTEF. This work was initiated by another Ph.D. student from our department; however the characterization of the devices remained to be done. In our work we continued this work, starting with visual characterization of the device, checking for errors in the process, but we did not find any. In particular we were worried about the two moving masses, because they may not have been completely released in the RIE additional process. For this reason, we placed the devices in buffered HF acid for removing the glass layer and then inspecting the silicon wafer (Figure 8). For electrical characterization of the accelerometer, they were mounted in a TO-8/600 header and tested by using a custom-made setup. The setup consisted of a shaker; a

reference accelerometer and a DAQ controller build in NI LabView software. The controller was able to control the shaker and generate vibrations at the desired frequencies.

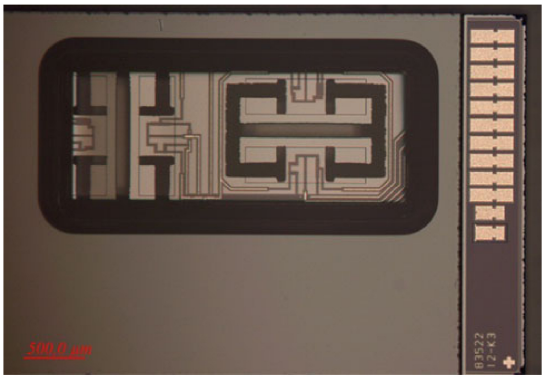

Figure 7. Accelerometer: top view picture.

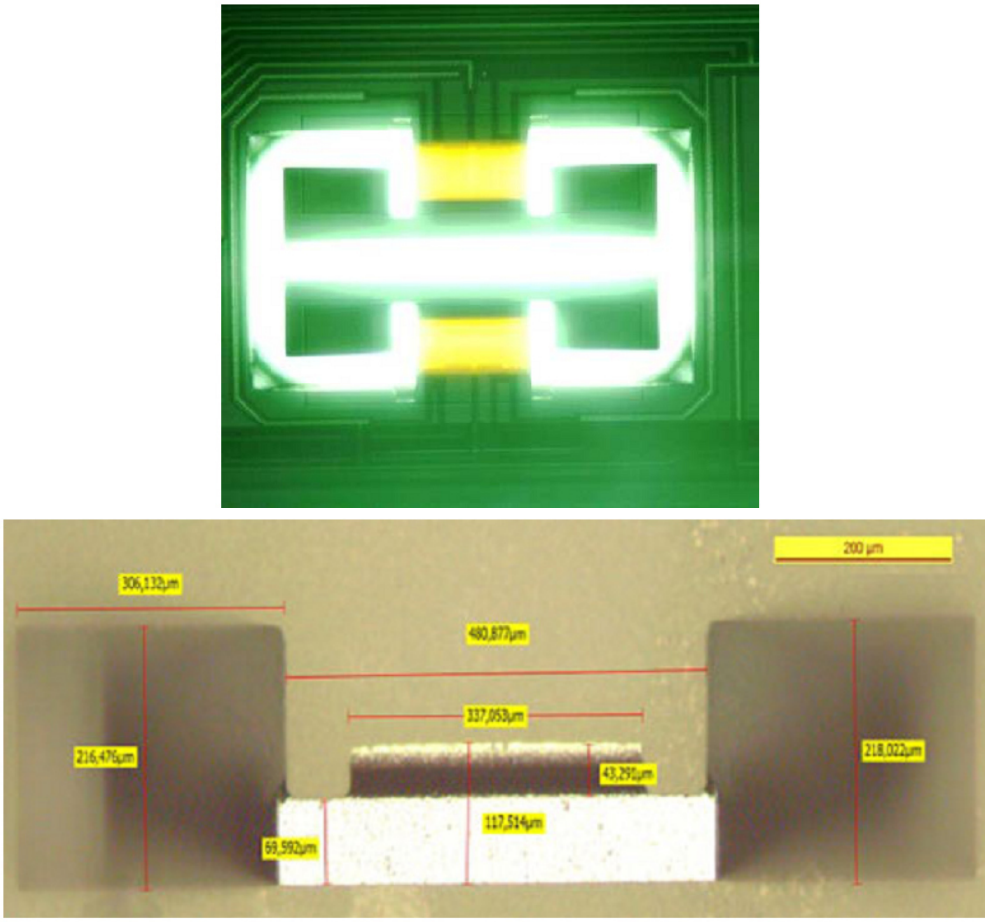

Figure 8. Optical inspection of the accelerometers: back illuminated device for checking the released structures and the beams (yellow); accelerometer mass.

We run vibration tests at 30 and 100 Hz, finding z-axis readout sensitivity before amplification to be around 0.04 [mV/V/g]. This low sensitivity value found on z-axis together with the high noise of the measurement system has made us investigate other commercial available solution for NAV vehicles such as the MPU9150 from Invensense used in the ELKA board (described in chapter 4).

2.3 Microphones

Beside accelerometers, we also investigated two types of microphones, originally developed for CO2 gas sensors elements [23]. Two types of microphones were fabricated; a circular thin membrane microphone and a thick square membrane microphone. Both versions were fabricated using the MultiMEMS process with piezoresistive sensing elements. Initial tests were performed by [23], however these tests were specifically made for low frequencies and thus we wanted to extend the characterization of the devices also into higher frequencies.

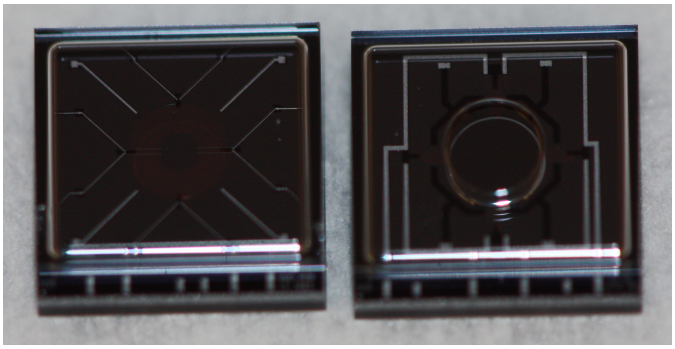

Figure 9. Thin membrane (left) and tick membrane (right) microphones.

We built a measurement set up similar to the one presented in [23], with better control and a more accurate signal processing, however we were unable to collect suitable data for publishing. This was mainly caused by the high noise from the measurement set up (especially in the low frequency range). Characterization of the sensors by building analytical model and a Finite Element Model (FEM) of the membranes has also been done to have a better understanding of the dynamics inside the devices. We started by simulating the microphones membranes by using COMSOL Multiphysics modelling software, using particular care to model the transition region between the thick-thin regions of the

membranes as shown in Figure 10. For reducing the computational complexity of the design we draw only a quarter of the membrane and then used the symmetry axis to mirror the structure.

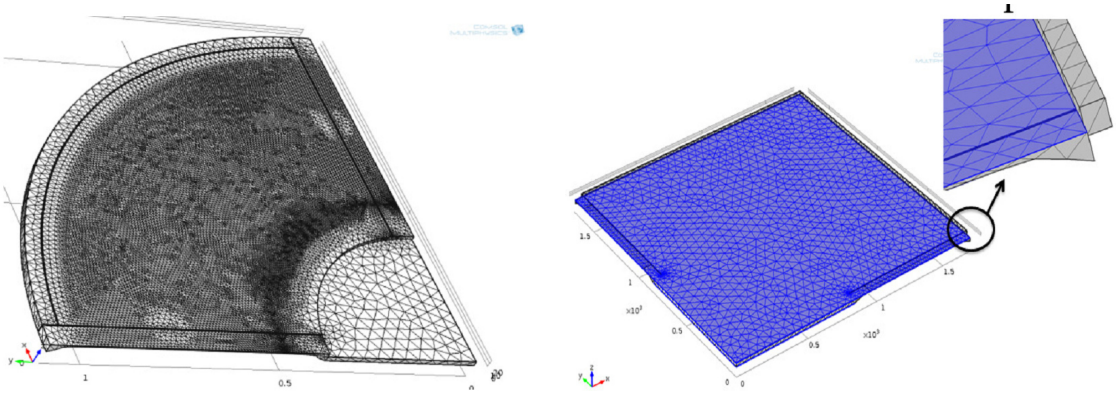

Figure 10. COMSOL model of the circular thin membrane (left) and square thick microphone membrane (right).

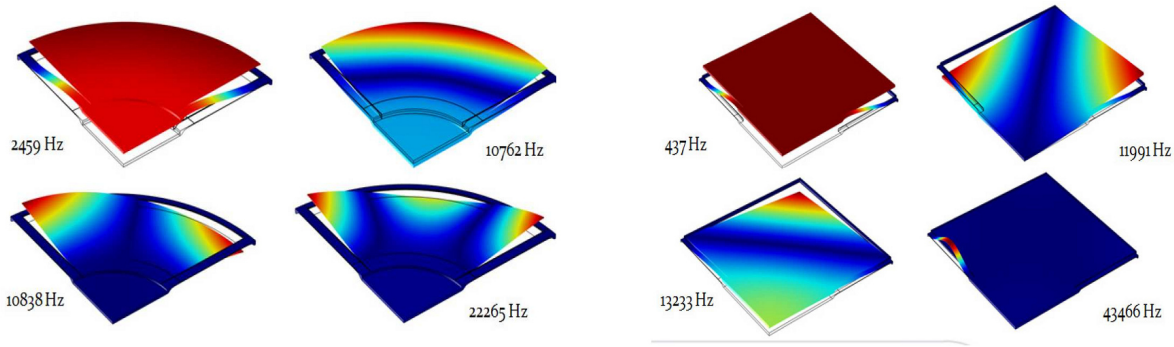

Figure 11. Eigen frequency of the round and square microphone membranes (COMSOL simulation).

For the analytical model, we wanted to estimate the effect of air going through the recess slid between the membrane and the frame, calculating response time for the cavity. We used a simple model consisting of a cavity with a membrane as shown in Figure 12. For the study we assumed that a $t=0^{+}$, a pressure P2 is applied from the external and a fluid flow Q start to stream inside the cavity. We also assumed that this change is much faster than the mechanical response of the system and thus modeled the membrane as a stiff wall (n is the number of moles).

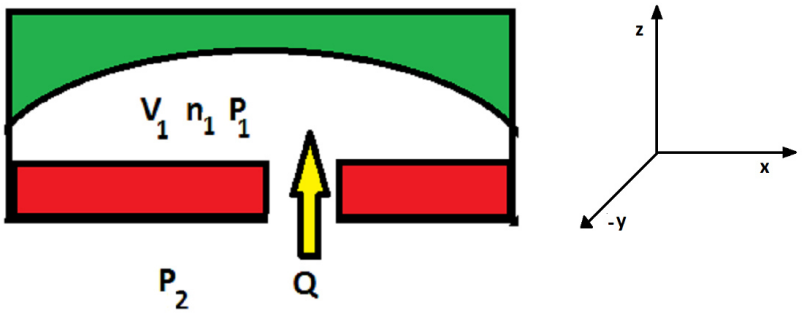

Figure 12. Membrane-cavity system.

We assumed that Q is a Poiseuille flow (no slippery boundary conditions) and is proportional to the pressure difference; furthermore we also assumed that the pressure P in the slid linearly decreases over the z axis. Based on these suppositions we estimated the time constant τ of the system, resulting as:

$$\tau = \frac{V_1 V_m h\ 12\eta}{rTwd^3} \qquad \{2\}$$

Where V_1 is the cavity volume, V_m is the molar Volume, η is the viscosity, T is the temperature, h, w and d are the dimensions of the slid. Substituting the values for each microphone, we found the time constant and the frequency cut off, shown in Table 1:

Table 1. Results for the two microphones.

	Circular membrane	Square membrane
Time constant (τ) [s]	$20 \cdot 10^{-6}$	$82 \cdot 10^{-6}$
Cut-off period (5τ) [s]	$100 \cdot 10^{-6}$	$410 \cdot 10^{-6}$
Frequency@5τ [Hz]	10000	2400

We found this result interesting since it shows the minimum working frequency. Indeed, if the external pressure changes are very slow (low frequency), the fluid will have time to "flow" inside the cavity thought the slid and thus the pressure difference applied to the microphone membranes becomes very small (reduced sensitivity). We also compared these results with the mechanical simulation outcomes and discovered that these devices may

have some designs problems. Indeed the mechanical resonance frequency (simulated with COMSOL) is below the cut off frequency calculated by the analytical model, giving a loss in performances (reduced sensitivity). The initial tests performed on these microphones, presented in [23] are not sufficient to give a complete understanding of the device and thus measurements with a different set up are needed for more direct comparison between analytical model and measurements.

3 Interconnections

Nowadays, many Micro and Nano Air vehicles include all the electronic circuitry in a single PCB (e.g. [8]). This is easy to achieve as the electronics onboard are relatively simple and only include the basic functions. However, for more advanced applications, multiple boards may be required onboard. For example, one board control the flight of the aircraft and in a separate board, there is the entire digital signal processing for the camera(s) and other payload sensors and/or RF circuitry. The idea of stacking PCBs onto each other may help to shrink the vehicles further, making the footprint smaller and using space otherwise left unused. Unfortunately, PCB to PCB Interconnections are among the areas that are least optimized for low weight applications. Current existing solutions can be divided into two classes:

- Cables.
- Connectors.

These existing solutions may be a limitation when used onboard in Nano Air Vehicles, because their intrinsic large footprint and the requirement of extra mechanical support for the PCBs. In this chapter we present a simple and reliable solution for PCB to PCB interconnects.

3.1 Cables and Connectors

Cables represent a common method for connection between two or more PCBs. It is used in many applications, from personal computers to mobile phones. It is a cheap and reliable solution that allows boards to be connected over relative large distances. It is simple to install and normally can be readapted to a new configuration without problems (changes on PCB orientation, positions etc.). They exist in many different dimensions, depending on the application. Two important characteristic is the number of wires and the minimum centre distance between them (pitch). Other important parameters are the

type/size of core and insulator. For low weigh applications (such as the connection between the main board and LCD screen in mobile phone), the configuration normally consists of a flexible flat cable (FFC), with a high number of wires and a low pitch. FFC can reach a pitch as low as 0.3 mm (such as the Axojump® Flat Flexible Cables from Hiconnex [25]) or has more than 100 wires (such as the 3754 Series from 3M [26]). Even though the cable can have very low weight, it does not provide sufficient mechanical support for PCBs and thus a complete system will always need an extra support frame for the boards. This frame can take a lot of space and add several grams to the final system weight that can be extremely disadvantageous.

The other alternative is connectors. This system is in general made of plastic with metal spikes. Despite their pitch being very small, they are in general heavy and require a large footprint on the board especially for high number of contacts. Furthermore, they can provide a sort of mechanical connection, however this is not reliable enough for holding the two PCBs in place, therefore they still require extra frame support.

A more common solution consists of having a combination of cables and connectors. This will however add even more weight to the system and should not be pursued for Nano Air Vehicles.

3.2 Interposer Technology

For overcoming the limitations presented in the previous paragraph, we investigated a new solution that allows for having mechanical and electrical connection at the same time.

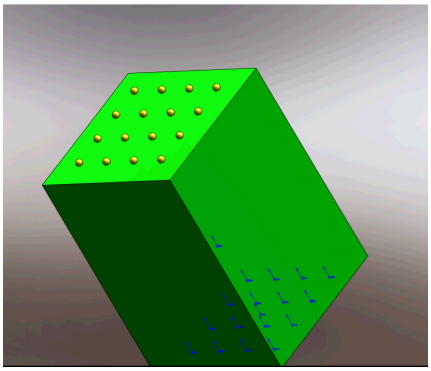

Figure 13. Interposer with vias: graphic model.

It consists of a small spacer with conductive VIAs (Figure 13) to be placed in between two PCBs as shown in Figure 14. The interposer is designed to:

- Build a reliable electrical and mechanical interconnection.
- Leave enough space between the two boards for electronic component placements.
- Keep the weight and size as low as possible.

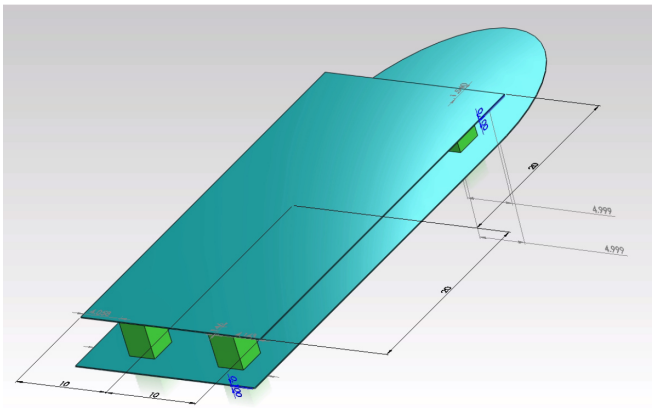

Figure 14. Interposer mounted between two PCBs. The top PCB is mechanically and electrically connected to the bottom PCB.

For the fabrication process we had to select spacer material, hole drilling technique and via filling metal. We decided to fabricate our interposer by using standard PCB technology in order to keep the cost low. The original design consisted of a via array with a pad directly onto each via. Unfortunately, not one of the contacted PCB manufacturers was able to fill the holes with conductive material and build a pad directly onto it, so we evaluated different designs. Our first alternative consisted of a blinded via and a pad shifted as shown Figure 15.

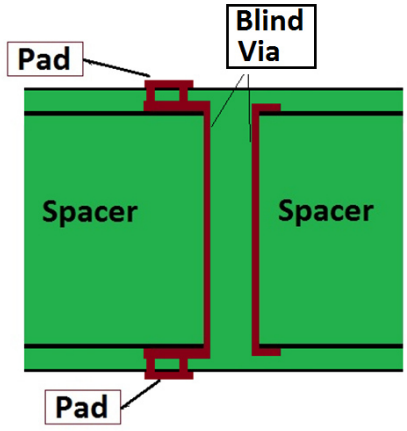

Figure 15. Blind via solution.

However, this solution was complicated and costly to fabricate because of the presence of blinded vias and multiple PCB layers. An alternative and easier solution was found by only shifting the VIA array a few hundred microns to 45° angle as shown in Figure 16.

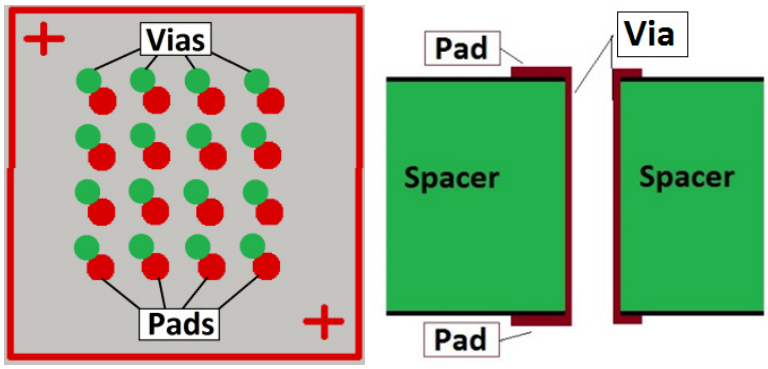

Figure 16. Top view and cross section view of the interposer.

Together with this solution we also fabricated two different PCBs for testing the final systems: The larger one (12x12 mm) to be used as bottom substrate and a smaller one (5x5 mm) to be flipped and attached on top of the structure (with the spacer in between the stack).

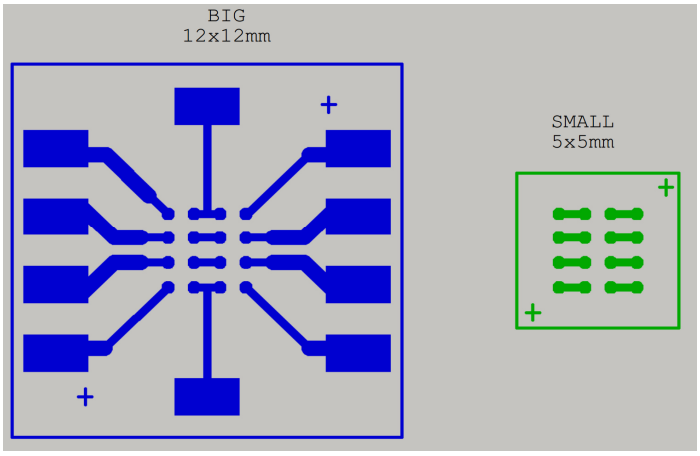

Figure 17. Big and small test PCBs.

By using this method we were able to create four electric chains for easy testing. Each chain included 8 interconnections, 4 vias and about 1 cm of track. Furthermore for the first and the last chain, we were also able to check half of it.

The samples were fabricated in standard FR4 and attached by using Lead Based solder paste (of Sn62Pb36Ag2 alloy). In particular, we manually dispensed the paste onto the two PCB pads, we created the stack and then we reflowed it in the oven. Final system is shown in Figure 18.

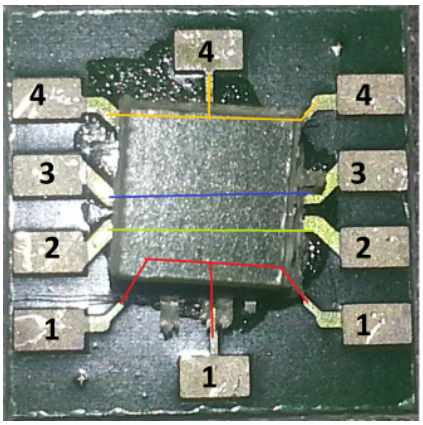

Figure 18. Final system. The conductive chains are highlighted with colours.

3.2.1 Interposer Tests and Results

Vibration tests and thermal cycling tests were performed to evaluate the reliability of the system created. For the vibration tests we used a "Bruel and Kjaer Vibration Exciter Type 4809" controlled by a virtual signal generator program using a NI-DAQ board. The samples where mounted onto the shaker by mechanical attaching the Big PCB onto the vibrating shaft. The samples were divided into two groups: One excited in the transversal direction (x-axis) and the second one in the normal direction (z-axis) as shown in Figure 19.

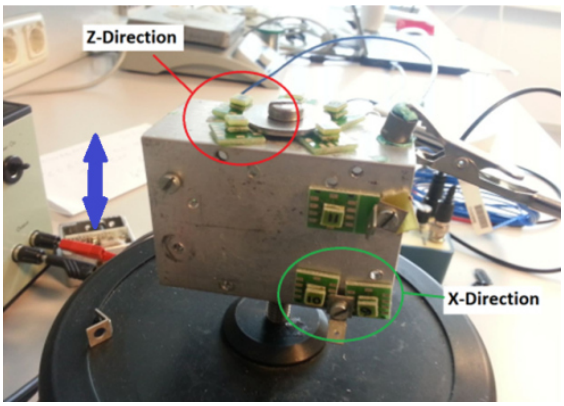

Figure 19. Samples attached to the shaker.

The samples were then tested at frequencies between 50 and 500 Hz, with 1 Hz frequency steps. We performed four sweeps at different acceleration rates. Each sweep lasted 19 minutes and the electrical resistance in between each sweep was measured. Furthermore, because of the instability of the shaker, we also recorded the acceleration profiles (reported in Paper III). However, for increasing the shear stress to the system, in the last two vibration sweeps we added 1g extra mass (made by lead) on top of the structure as shown in Figure 20. In this last configuration we experienced failures on 4 different chains.

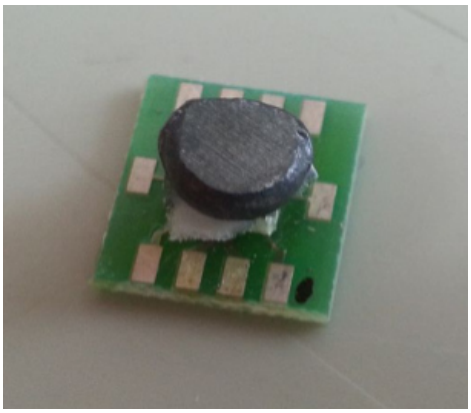

Figure 20. 1 g extra mass added onto the structure.

Beside vibration test, we also performed thermal cycling tests. Those tests were implemented in accordance with the military standard 883 method 1010.8, which regulates the boundary conditions for thermal testing in military components qualifications. In particular we executed 11 thermal cycles from +150ºC to -65ºC. The total test endured for around 24 hours. The results from both the vibration tests and the thermal cycling test are very encouraging since they do not show any joint degradation. We found an average chain resistance of 24 mΩ which is in line with other solder techniques. Furthermore, the maximum variation of the resistance distribution after the tests is always less or equal to 4mΩ. We believe that this small variation is mainly caused by the inaccuracy of the measurement set up rather than an actual joint degradation. A more complete overview of all the results can be found in the paper IV.

4 The Autopilot

The autopilot system mounted on a NAV has to perform multiple tasks such as to help the pilot to stabilize the flight, read and process sensor data, send and receive information from/to the Ground Base Station (GBS), control actuators etc. Despite the name, the system is not designed for being fully autonomous, but rather to assist the pilot during the flight. In other word, the vehicles are not able to select optimal trajectories or to take decision; for these assessments, they still rely on user's commands. Trajectory control can be added by upgrading the firmware.

Autopilots on NAVs are similar to the one used in larger vehicles, with the extra requirement of fulfilling low power and low weight constrains. As reported in [2], general weight budget for electronics onboard of a NAV is around 2 g. This includes navigation sensors, microcontroller unit and RF transmission interface. Furthermore it may also include extra sensors such as cameras, GPS, gas sensors, biological sensors, etc. Unfortunately, because of these very high constrains, the availability in the market for a small autopilot system is limited. One solution that fulfills these requirements is the "Guidance and Inertial Navigation Assistant" (GINA), developed from Berkeley University for small robotic applications. The latest version (2.2) released in 2010 [28] includes 9 axis inertial sensing provided by 4 MEMS devices. One gyroscope detects Pitch Roll and Yaw angular rates, while two 3D accelerometers are used for sensing the linear rates. The core consists of MSP430 from Texas Instrument, which is a 16-bit microcontroller, part of the MSP430F2xx family. It supports up to 16 MHz operation. Together with the processing unit, the GINA board also includes Wi-Fi Interface (AT86RF231 from Atmel Corporation) and the possibility to add a chip antenna onboard. Despite that this board is relative small (2.5 cmx2.5 cm area) and that it is relative light weight (1.7 g), the design is already more than 3 years old and thus some components such as the accelerometer and the gyroscope are outdated. Furthermore, a 16-bit microcontroller may be a limitation for some of the

more advanced computations. Based on these shortcomings, we decided to develop our own autopilot system. This new system had to be optimized for small flying vehicles. However we also wanted to be hardware independent from the vehicle configuration and thus be able to control and vary the usage of copter configuration, from the standard two rotor copter to the more advanced and non-conventional design such as gyrocopters or octocopters, which may require up to 8 motors to be controlled at the same time. The system would also include all the smallest and most performing 3D gyroscopes, 3D accelerometers and 3D magnetometer available in the market, as well as a reliable 2.4 GHz transmitting interface. Particularly important was also the choice of the microcontroller, which needs to have enough calculation power to compute all the information directly on board of the vehicle. These features must all comply with the extremely low power, size and weight budget requirements for such vehicles.

The University of Maryland (UMB), in College Park, U.S.A. (they are currently a GINA users) was particularly interested in developing a new autopilot hardware platform. From the collaboration between HiVe and UMB, a new autopilot system was designed, fabricated and successfully tested; this new system was called Embedded Lightweight Kinematic Autopilot (ELKA).

4.1 ELKA Design and Fabrication

The new board had to be designed to be used onboard for small flying vehicles, where size and weight matter more than extra functionalities. As a reference point, we used the GINA board; so we set the target for ELKA to be at most the same size and weight as of GINA. We chose this goal for two reasons:

1. Since this was our first attempt to create an autopilot, in case of malfunctioning we wanted to have enough physical space for debugging and finding/fixing problems. This became more difficult as the dimensions shrink down.

2. Even with the same size and weight, the ELKA board has multiple advantages with respect to GINA, especially in performances as shown in Table 2.

Table 2: GINA versus ELKA Comparison (*estimation).

	GINA	**ELKA**
Nº Chips used (IMU+RF+μC)	6	3
Transmission range [m]*	20	80
Gyroscope spectral noise	0.03 ◦/sec	0.005 ◦/sec
Bits μC	16	32
Speed	16 MHz	72 MHz
RAM	8 kB	20 kB
ROM/FLASH	116 kB	128 kB

Our approach was to keep the design simple, removing all the unnecessary features onboard while leaving the possibility to still access them by external connectoction to the user. Furthermore, we also wanted flexibility and hardware independency, in order to use this board not only on a specific class of vehicles, but rather build one flexible circuits that could be easily adapted from ground vehicles to aerial vehicles to small robot. Communication was also an important part. We wanted the system to communicate at normal 2.4 GHz without adding any extra element onboard; so we included a chip antenna onboard, making ELKA ready to be used without any additional components.
The three basic blocks in ELKA are:

1. Microcontroller unit (μC).
2. 9-Axis Inertial Motion Unit (IMU).
3. RF Interface.

In addition, there is an extra block EXT representing the external connectors needed for accessing extra features of the board (Figure 21).

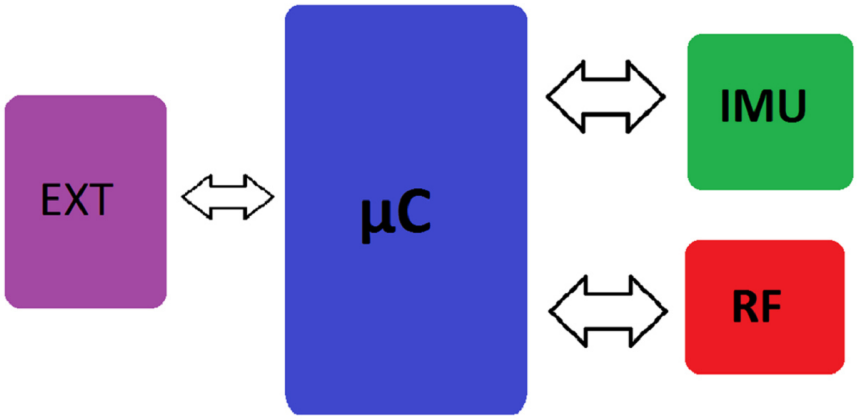

Figure 21. The ELKA board: block diagram.

The components of each section have been carefully selected among the smallest and most highly performing devices available in the market. For the microcontroller we chose the STM32F103CB, a 32-bit microcontroller based on the ARM CORTEX M3 core. In particular, the F103 is one of the high performance microcontrollers in the F1 family. The core works at 72 MHz, while the large memory available onboard (Flash memory up to 128 Kbytes and SRAM up to 20 Kbytes) allows storage of large programs and complex algorithms execution. The STM chip also offers two 12-bit ADCs, three general purpose 16-bit timers (4 channel each) plus one PWM timer, as well as advanced communication interfaces such as: two I2Cs, two SPIs and three USARTs [29]. The device accepts 3.3 V as supply voltage and it is available in the LQFP 48 package, which is the perfect tradeoff between size and number of pins for this application. The instruction set for the F1 family includes Thumb, Thumb-2 and Saturated Math. Regarding the IMU we selected a single chip that included all the required sensors. In particular, we chose the MPU9150 from InvenSense, which includes a 3D accelerometer, a 3D gyro and a 3D magnetometer. Furthermore it also includes a thermal sensor that could be used for compensating the thermal drift of the sensors. Having all the motion sensors in one chip provides several advantages: It requires less footprint on the board, saving weight and space, it helps to save power, since the power consumption of one single chip is in general lower than three discrete chips and the most important, it eliminates the misalignment error between gyro, accelerometer and magnetometers axis. The Gyro noise is 0.005 dps/√Hz and has user-

programmable full-scale range settings for the accelerometers and the gyroscopes. For the transmission we chose a single-chip very low power RF transceiver with a data rate up to 2 Mbit/s., everything packed in a QFN24 package (5x5mm). In Figure 22 the Elka final schematic is shown, while Figure 23 shows the final physical board (dimension 28x21mm^2, weight 1.2g) compared with a quarter of dollar.

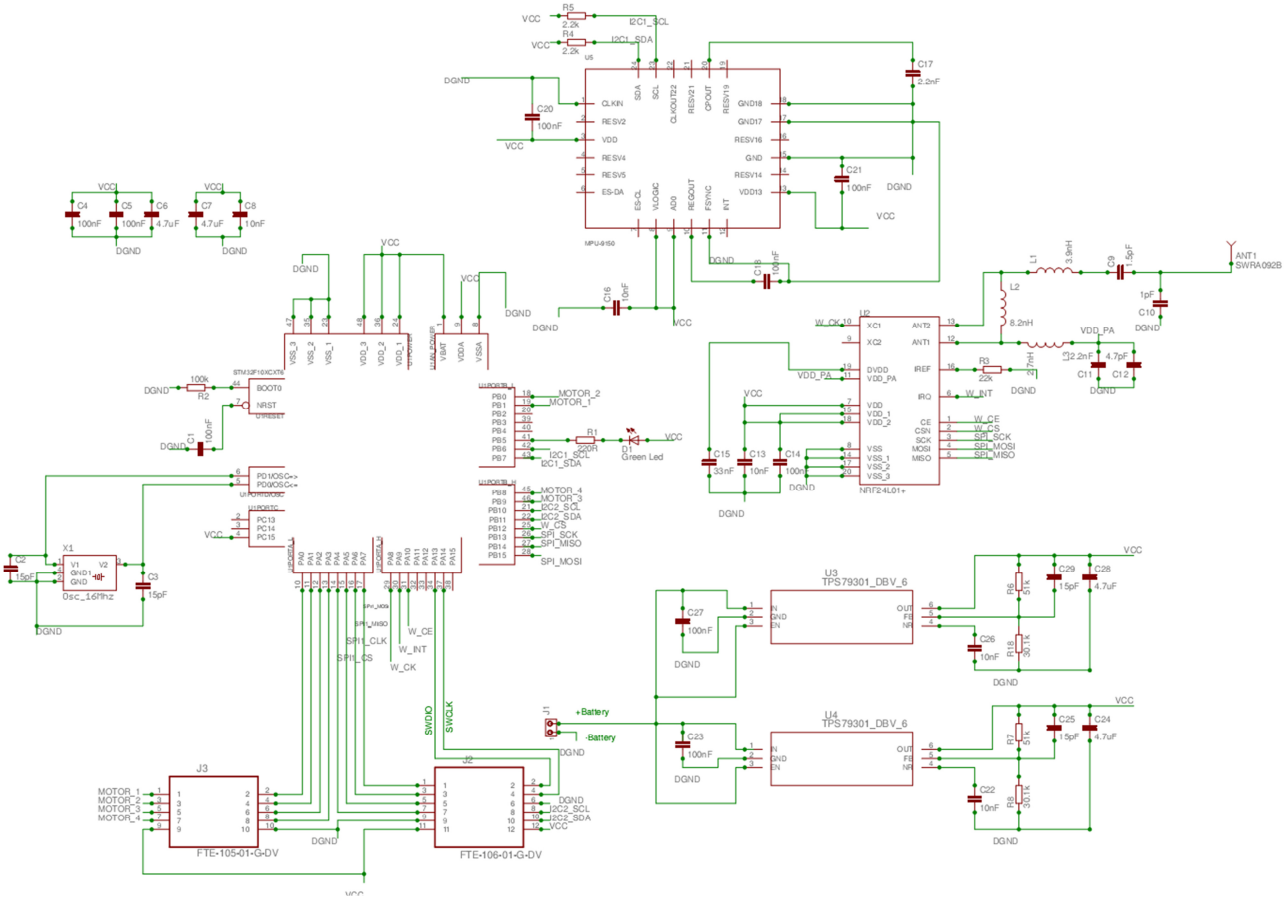

Figure 22. The Elka complete schematic.

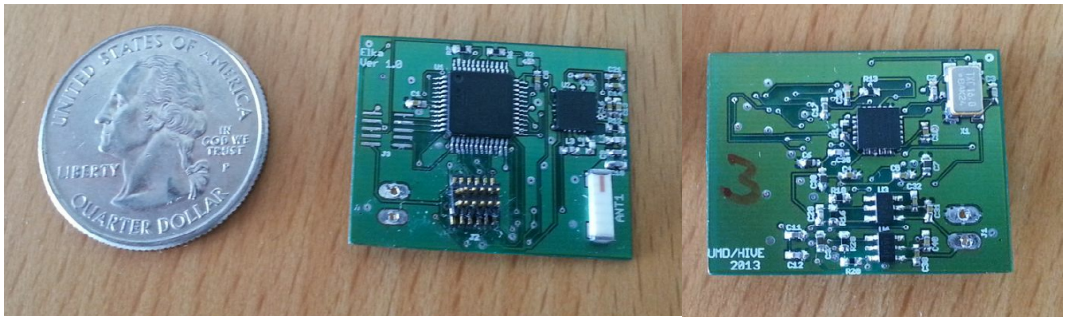

Figure 23. The fully assembled Elka Board compared with a quarter of dollar.

4.2 ELKA Tests

In order to test the ELKA board, we prepared several piece of C code. We used these small programs for checking the functionality of the board at hardware level. We ran many tests, from simple LED blinking until more complex and hardware demanding tasks. A few of the most significant tests are reported here. Among all the instruction used, we only reported the most important.

For the blinking led test, we wanted to check if the microcontroller was working properly and if we were able to flash the code inside microcontroller. For setting the GPIO we used:

```
GPIO_InitTypeDef gpio;
RCC_APB2PeriphClockCmd(RCC_APB2Periph_GPIOB, ENABLE); //Enable APB2 clock
GPIO_StructInit(&gpio);
gpio.GPIO_Pin = GPIO_Pin_5; // Green LED
gpio.GPIO_Mode = GPIO_Mode_Out_PP; // Push Pull output
gpio.GPIO_Speed = GPIO_Speed_2MHz;
GPIO_Init(GPIOB, &gpio);
```

While, for the actual blinking we used:

```
while(1)
 {
  for (i=0; i<1000000; ++i);
  GPIO_WriteBit(GPIOB, GPIO_Pin_5, led_state ? Bit_RESET : Bit_SET);
  led_state = !led_state;

}
```

where the “for” cycle is only used as a delay instruction.

Another test run was focused to test the IMU sensor and the I2C connectivity. The code for this test is much longer and more complex. Indeed for the I2C interface setup we used:

```
//Method for initialize I2C1
static void init_I2C1(void)
{
	GPIO_InitTypeDef GPIO_InitStructure;
	I2C_InitTypeDef I2C_InitStructure;
	RCC_APB2PeriphClockCmd(RCC_APB2Periph_GPIOB, ENABLE);
	RCC_APB1PeriphClockCmd(RCC_APB1Periph_I2C1, ENABLE);



	//setup SCL and SDA pins
	GPIO_StructInit(&GPIO_InitStructure);
	GPIO_InitStructure.GPIO_Pin = GPIO_Pin_6 | GPIO_Pin_7;
	GPIO_InitStructure.GPIO_Speed = GPIO_Speed_50MHz;
	GPIO_InitStructure.GPIO_Mode = GPIO_Mode_AF_OD; // open drain
	GPIO_Init(GPIOB, &GPIO_InitStructure);

	/* Configure I2Cx */
	 I2C_DeInit(I2C1);
	 I2C_InitStructure.I2C_Mode = I2C_Mode_I2C;
	 I2C_InitStructure.I2C_DutyCycle = I2C_DutyCycle_2;
	 I2C_InitStructure.I2C_Ack = I2C_Ack_Enable;
	 I2C_InitStructure.I2C_AcknowledgedAddress = I2C_AcknowledgedAddress_7bit;
	 I2C_InitStructure.I2C_ClockSpeed = 100000;
	 I2C_InitStructure.I2C_OwnAddress1 = 0x00;
	 I2C_Init(I2C1, &I2C_InitStructure);
	 // init I2C1 enable I2C1
	 I2C_Cmd(I2C1, ENABLE);
}
```

While for the sending and receiving data, we implemented a function readx: with this program, we were able to read sensors data form IMU, for a later onboard processing.

```
int16_t* readx(I2C_TypeDef* I2Cx, uint8_t address){
	static int16_t id[7];
	int j;
	I2C_startslave(I2Cx, address); //enable the ACK and send the start signal
and address the slave
	I2C_send(I2Cx, address); //send the byte to the slave (it need I2C_start
before)
    /* generate start signal */
	I2C_startsign(I2Cx);
	I2C_setreceiver(I2Cx, address); //set the I2C in mode Receiver
	   uint8_t id1=I2C_read(I2Cx);  //ax out h
	   uint8_t id2=I2C_read(I2Cx);  //ax out low
	   uint8_t id3=I2C_read(I2Cx);  //ay out h
	   uint8_t id4=I2C_read(I2Cx);  //ay out low
	   uint8_t id5=I2C_read(I2Cx);  //az out h
```

```
        uint8_t id6=I2C_read(I2Cx);  //az out low
        uint8_t id7=I2C_read(I2Cx);  //temp out h
        uint8_t id8=I2C_read(I2Cx);  //temp out low
        uint8_t id9=I2C_read(I2Cx);  //gx out h
        uint8_t id10=I2C_read(I2Cx);  //gx out low
        uint8_t id11=I2C_read(I2Cx);  //gy out h
        uint8_t id12=I2C_read(I2Cx);  //gy out low
        uint8_t id13=I2C_read(I2Cx);  //gz out h
        uint8_t id14=I2C_read(I2Cx);  //gz out low


        I2C_stop(I2Cx);

        id[0]=(id1<<8)|id2;
        id[1]=(id3<<8)|id4;
        id[2]=(id5<<8)|id6;
        id[3]=(id7<<8)|id8;
        id[4]=(id9<<8)|id10;
        id[5]=(id11<<8)|id12;
        id[6]=(id13<<8)|id14;
        return &id[0];
}
```

An extension of this code was meant to extract the Eulerian angles from the accelerometer and gyroscope values (by using quaternion estimation computed from gradient-descent based methods) and print it on the screen by using a USART interface. With a simple Visual Python script we were able to recreate a virtual version of the board, showing ELKA orientation in real-time.

The last two tests reported here were focused on evaluating the Timers/PWM and the wireless transceiver. For the first test, we used a servomotor as shown in Figure 24. The motor motion was modulated by the IMU reading values and was thus moving according to the board orientation.

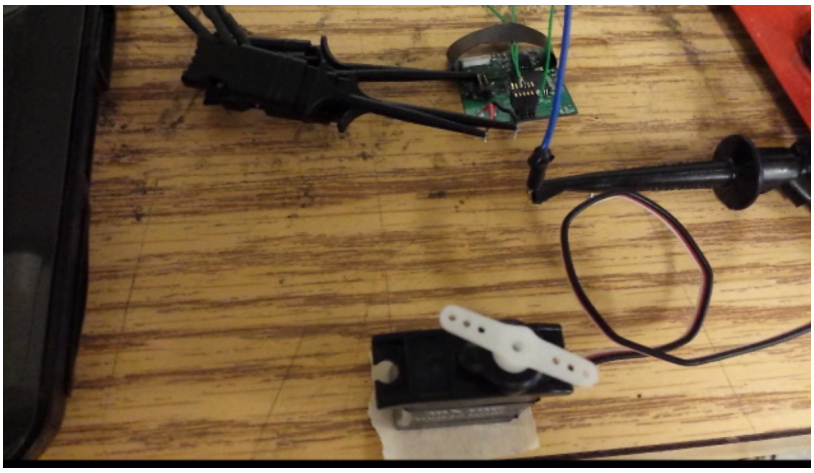

Figure 24. Servo motor attached to ELKA board.

The last test was focused on establishing and transferring data by a wireless interface. For doing that, we created another circuit to be used as receiver node. The new circuit, built on a breadboard, included the STM32 discovery with an external NRF24l01+ interface. The board was then connected to the PC by using USART interface. Since ELKA has the NRF chip on the SPI interface, we had to write the code to initialize such a connection with:

```
void SPI2_Init(void)
{       int j;
        SPI_InitTypeDef   SPI_InitStructure;
        GPIO_InitTypeDef      GPIO_InitStructure;

RCC_APB2PeriphClockCmd(RCC_APB2Periph_GPIOA | RCC_APB2Periph_GPIOB, ENABLE);
RCC_APB2PeriphClockCmd(RCC_APB2Periph_AFIO, ENABLE);
             GPIO_InitStructure.GPIO_Pin = GPIO_Pin_8;
             GPIO_InitStructure.GPIO_Mode = GPIO_Mode_AF_PP;
             GPIO_InitStructure.GPIO_Speed = GPIO_Speed_50MHz;
             GPIO_Init(GPIOA, &GPIO_InitStructure);

RCC_MCOConfig(RCC_MCO_HSE);
RCC_APB1PeriphClockCmd(RCC_APB1Periph_SPI2, ENABLE); //enable spi2 clock.
       GPIO_InitStructure.GPIO_Pin = GPIO_Pin_13 | GPIO_Pin_15; //B13=clk
B15=MOSI
       GPIO_InitStructure.GPIO_Mode = GPIO_Mode_AF_PP;
       GPIO_InitStructure.GPIO_Speed = GPIO_Speed_50MHz;
       GPIO_Init(GPIOB, &GPIO_InitStructure);
       GPIO_InitStructure.GPIO_Pin = GPIO_Pin_12;// CSN= chip select PIN B12
       GPIO_InitStructure.GPIO_Mode = GPIO_Mode_Out_PP;
       GPIO_InitStructure.GPIO_Speed = GPIO_Speed_50MHz;
        GPIO_Init(GPIOB, &GPIO_InitStructure);
```

```
        //CE
        GPIO_InitStructure.GPIO_Pin = GPIO_Pin_10; // CE= chip enable PIN A10
        GPIO_InitStructure.GPIO_Mode = GPIO_Mode_Out_PP;
        GPIO_InitStructure.GPIO_Speed = GPIO_Speed_50MHz;
        GPIO_Init(GPIOA, &GPIO_InitStructure);
        //IRQ
        GPIO_InitStructure.GPIO_Pin = GPIO_Pin_9; //IRQ = PIN A9
        GPIO_InitStructure.GPIO_Mode = GPIO_Mode_IN_FLOATING;
        GPIO_InitStructure.GPIO_Speed = GPIO_Speed_50MHz;
        GPIO_Init(GPIOA, &GPIO_InitStructure);

        //MISO
        GPIO_InitStructure.GPIO_Pin = GPIO_Pin_14; //MISO = PB14
        GPIO_InitStructure.GPIO_Mode = GPIO_Mode_IN_FLOATING;
        GPIO_InitStructure.GPIO_Speed = GPIO_Speed_50MHz;
        GPIO_Init(GPIOB, &GPIO_InitStructure);

         /* SPI2 configuration */
         SPI_InitStructure.SPI_Direction = SPI_Direction_2Lines_FullDuplex;
         SPI_InitStructure.SPI_Mode = SPI_Mode_Master;
         SPI_InitStructure.SPI_DataSize = SPI_DataSize_8b;
         SPI_InitStructure.SPI_CPOL = SPI_CPOL_Low;
         SPI_InitStructure.SPI_CPHA = SPI_CPHA_1Edge;
         SPI_InitStructure.SPI_NSS = SPI_NSS_Soft;
         SPI_InitStructure.SPI_BaudRatePrescaler = SPI_BaudRatePrescaler_64;
         SPI_InitStructure.SPI_FirstBit = SPI_FirstBit_MSB;
         SPI_InitStructure.SPI_CRCPolynomial = 7;
         SPI_Init(SPI2, &SPI_InitStructure);
         /* Enable SPI2   */
         SPI_Cmd(SPI2, ENABLE);
}
```

An extra portion of code was added for sending byte through this link. We were able to transmit packages containing multiple bytes (numbers and letters), between the two boards. Furthermore we also set ELKA as receiver and the Discovery board as transmitter, being able to establish a bidirectional connection.

5 Energy Storages

In the last ten years, we have seen an exponential growth of portable equipment. Laptops, tablets, smartphones and portable game consoles are only a few examples of commercial devices that need an efficient energy storage system on board. Similar to the previous applications, NAVs also need an effective power source, with the difference that it must be optimized for ultra-low weight budget. Indeed in a vehicle of 15 g, the energy storage system should take less than 50% of the total weight [2]. Batteries are nowadays the most used system; however, they are not very efficient. We accept their limitations (such as short lifetime, long recharge time, etc.) simply because there are no real alternatives. An "ideal" battery should be light, have high energy density, high power density, infinite lifecycles and be fully recharged in a few seconds. Research in this field is divided in two main trends: the first one is focused to increase battery efficiency while a second one is investigating new and more disruptive alternative solution. Some examples of these promising substitutive energy storage systems, which in the future could replace battery are given by fuel cells, micro-turbines and supercapacitors.

Nano technology can provide an important contribution to this research, in particular regarding supercapacitors. These system are similar to the standard capacitors, but with a much higher capacitance. The basic structures consist of two electrodes and one dielectric material in between. Depending on the electrodes and dielectric material, they can be divided into three categories:

1. Electric Double Layer Capacitors (EDLC).
2. Electrochemical Pseudo Capacitors (EPC).
3. Hybrid Supercapacitors.

Among the three classes, EDLC is most similar to standard capacitors. They are called "Non Faradaic", because they do not involve any electrode-electrolyte charge transfer. The energy is stored in a pure electrostatic form and thus the capacitance is directly proportional to the electrodes area. For this reason, electrodes consist of materials that have a large surface such as carbon nanotubes or activated carbon. When compared with the other classes, this type of device offers a high power density but a low energy density.

The second supercapacitors class is the EPCs, which are called "Faradaic". Indeed, in this case the storage mechanism involves charge transfer between electrode and electrolyte. This process may be achieved in three different manners:

- Rapid and reversible Red-Ox reactions between the electrodes and the electrolyte.
- Surface adsorption of ions from the electrolyte.
- Doping and undoping of active conducting polymer material of the electrode.

The capacitors of this class have a high energy density but a low power density.

The last class is the hybrid supercapacitors, which try to combine both the advantages of EDLC and EPC. The basic idea is to use a combination of electrode materials used in EDLC for obtaining high power density and in EPC for increasing the energy density.

In this work we started a partial design of a new type of supercapacitor based on black silicon. Unfortunately the work has not yet been completed because of some technical problem in the ALD deposition.

5.1 Black Silicon Supercapacitor

When the smooth surface of a silicon wafer is machined to form a needle-shaped surface (Figure 25), the resulting structure is called "black silicon". The name derives from the property of this surface to absorb almost all the incident light, appearing to be black in colour when observed at the microscope. This structure has a very high active area and thus may be suitable for the creation of supercapacitors.

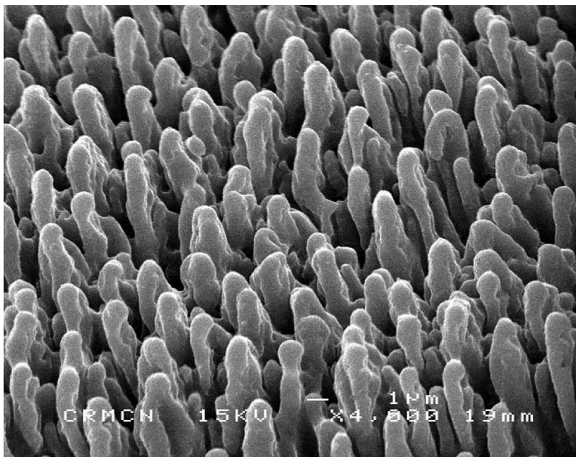

Figure 25. Black silicon structure **[31]**.

The process we wanted use is shown in Figure 26. It starts with a high doped silicon wafer, which will be the first capacitor plate.

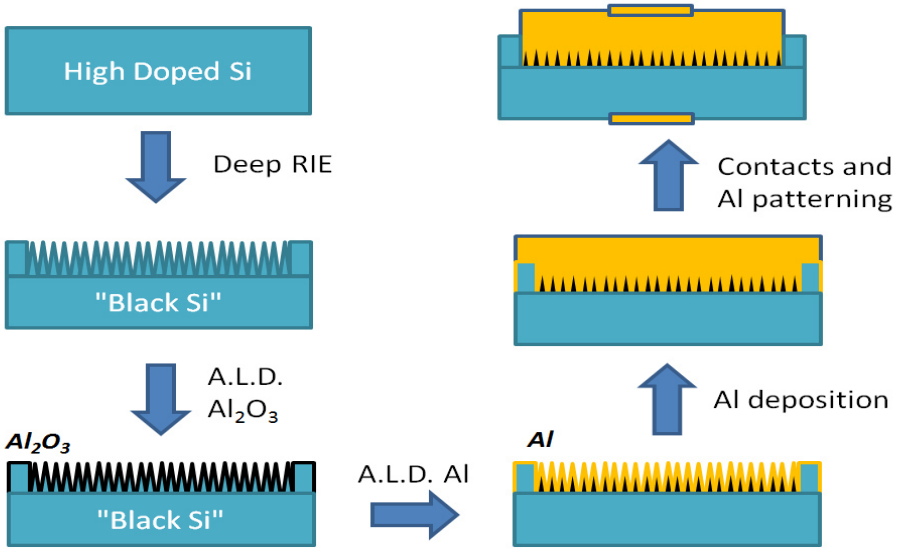

Figure 26. Black silicon supercapacitor: process overview.

The doped silicon surface is then machined by DRIE etch process that creates the needle-shaped surface structure ("black silicon"). By doing this we increase the active area of the plate and thus also its potential capacity (C) and energy stored (E) as shown in {3} and {4}

$$C = \varepsilon \frac{A}{d} \qquad \{3\}$$

$$E = \frac{1}{2} C V^2 \qquad \{4\}$$

Where d is the distance, ε is the dielectric constant and V is the voltage across the capacitor plates. The process continues by depositing a few nano-meters of oxide or dielectric

material by using atomic layers deposition (ALD) that will form the insulating layer of the capacitor. Example of this material could be Al_2O_3. This step is followed by a second ALD deposition of metal (e.g. aluminium) for creating a uniform conductive layer onto the oxide layer.

Once the basic capacitor structure is formed, we can then evaporate/sputter a thick deposition of the same metal, forming the second capacitor plate. It is important to remark that the second ALD process (Aluminium) is needed because evaporation/sputtering may be not sufficient to deeply penetrate between the spikes and thus is not able to uniformly cover the oxide layers, leaving bubbles that reduce the capacitance.

The final step involves Al patterning for releasing the contact pads on both silicon side and aluminium side.

Unfortunately, our laboratory does not have any equipment neither for creating the "Black Silicon", nor for making the Atomic Layer Deposition; so we set up some collaborations with "Technische Universitaet Ilmenau" in Germany that were able to provide black silicon wafer and Oslo University for the atomic layer deposition process.

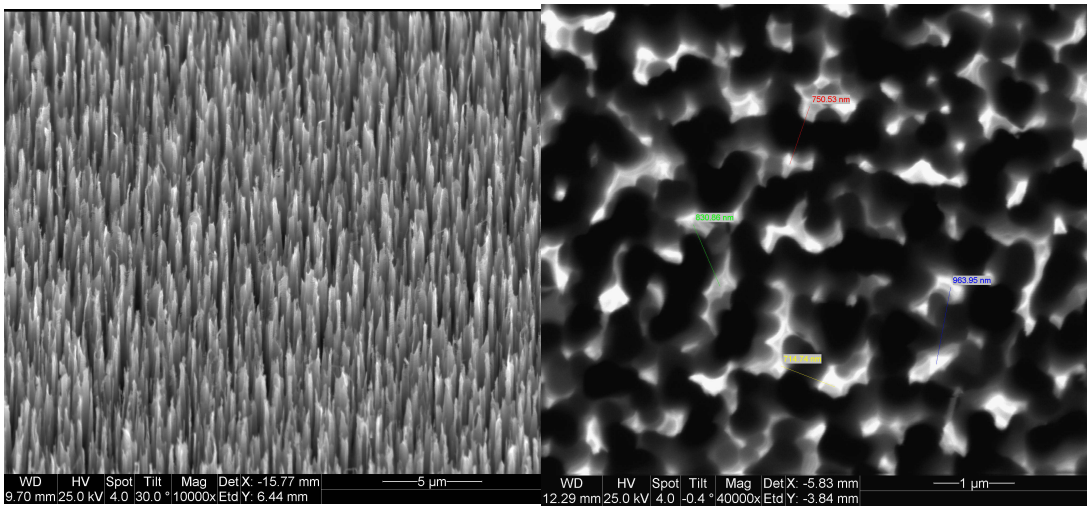

Figure 27. Black silicon wafer created in University of Ilmenau.

Since we also wanted to study the variation of capacitance when varying the resistivity of one plate, we ordered two different wafers with different resistivity values. The complete propriety list is summarized here:

Wafer 1: 100 mm diameter, (100) orientation, 525 µm thick, DSP, 1 – 10 Ωcm, n-doped (P).

Wafer 2: 100 mm diameter, (111) orientation, 400-440 µm thick, SSP, 0.017-0.025 Ωcm, n-doped (Sb).

The received wafers were then inspected by SEM microscope at different angles and magnitudes as shown in Figure 27. The spikes are around 100-200 nm in diameter, with an average distance between peaks of 400-600 nm. We believe that this structure is suitable for our purposes.

The wafer were subsequently shipped to Oslo University for creating the ALD structures, however their ALD process is currently not able to deposit metals and thus this project is not finished yet. An upgrade of their system for metal deposition should be available in early 2014 and this work will be followed by other HiVe researchers.

6 Concluding remarks and future prospective

Nano Air Vehicles will play an important role in our future. They will be adopted for many applications: from assisting soldiers in battlefields to search for survivors in rescues operations. In this Ph.D. work we identified the main parts of the existing vehicles and tried to find innovative solution to overcome the existing problems. The work done covered most of the key areas: Electronic, interconnections, sensors and energy storage.

In particular, I investigated the possibility to use piezoresistive devices for both navigation and payload sensors. From the measurements and models done, I concluded that, despite the possibility to create piezoresistive motion sensors and microphones with the MultiMEMS process, their sensitivity is too low for compete with commercially available solutions.

This Ph.D. continued by developing a simple and reliable interconnection solution between PCBs by using a small interposer. This spacer provides mechanical and electrical connection at the same time, reducing weight and space of the vehicles.

Furthermore, from the collaboration with the University of Maryland in USA, I also designed, fabricated and tested one of the smallest autopilot systems in the world (ELKA). The board is mainly focused for use in aerial vehicles; however, thanks to its combination of high computation power, low weight, small size and great hardware flexibility, it can be easily adapted to similar systems such as small robots or ground vehicles.

This thesis also presented the initial work done on black silicon supercapacitors. We established collaboration with two universities in Oslo (Norway) and Ilmenau (Germany) and we successfully fabricated two different black silicon wafers with different resistivity. The work has not been completed, however it is planned to be followed up by other researchers in 2014.

The future trend for these vehicles will be driven by integration. Upcoming vehicles will have a complete set of sensors and actuators onboard and they will be able to perform many

different missions; not only sensing, but also picking up material samples, releasing small amount of substances or sending RF commands for controlling larger actuators. At the same time, they will also get smarter; being able to take autonomous decisions and perform swarm operations. They will probably be able to track and follow patterns and/or decide best strategies in different situation without any human help (choose the best route, decide when to release wireless sensors, etc.). If the autopilot software gets more advanced, they will also be able to automatically patrol boundaries, perimeters of tactical buildings etc., with automatic return to base-station for recharging batteries (if batteries are still used!). They will be able to recognize threats and act accordingly for example by alerting the main operation central. Energy storage will be the main bottleneck for the vehicles. Current batteries give around 30 minutes autonomy. Even if research improves them by 10%, autonomy will only gain 3 minutes more. For this reason, it is essential to find alternatives to this energy source. In case of indoor flight, one important challenge in navigation should be addressed. Large drift in inertial motion sensors create a growing error in the calculated position. Current vehicles use GPS for periodical recalibrations. However, in case of indoor flight, this is often not possible because of lack of GPS signals, thus their maneuverability will become more difficult. For overcoming this, it is important to reduce current gyroscope/accelerometer noise and finding alternative ways for recalibration. Indoor flights also create a problem in communications where the trade-off between transmission range, bitrate, frequency and antenna size increases in difficulty. In this case new MEMS filters and resonators may help to reduce the power usage and minimize space and weight.

Luckily, most of these challenges are not NAV specific, but are common with other fields. Smartphones will continue to push research in many ways, from new and more efficient batteries to low cost sensors. Thanks to the high investments done every year, I expect that most of the main challenges will be addressed in a relative short time period.

Bibliography

[1] DARPA. [Internet]. Available: www.darpa.mil.

[2] L. Petricca, P. Ohlckers og G. Christopher, «Micro- and Nano-Air Vehicles: State of the Art,» *International Journal of Aerospace Engineering,,* 2011.

[3] «Nano-air vehicles: small eyes in the skies,» [Internet]. Available: http://www.airforce-technology.com/features/featurenano-air-vehicles-small-eyes-in-the-skies. [5 2013].

[4] DARPA, «Nano Air Vehicles Program,» DARPA, [Internet]. Available: http://www.darpa.mil/Our_Work/DSO/Programs/Nano_Air_Vehicle_(NAV).aspx. [05 2013].

[5] «Black Hornet: British Army unveil latest weapon against the Taliban,» The Telegraph, [Internet]. Available: http://www.telegraph.co.uk/news/uknews/defence/9869468/Black-Hornet-British-Army-unveil-latest-weapon-against-the-Taliban.html. [5 2013].

[6] «Black Hornet spycam is a 'lifesaver' for British troops.,» BBC, [Internet]. Available: http://www.bbc.co.uk/news/uk-21450456. [2013].

[7] Prox Dynamics, «Black Hornet,» [Internet]. Available: http://www.proxdynamics.com/products/pd_100_prs/. [5 2013].

[8] Bitcraze, «Crazyflie,» 08 2013. [Internet]. Available: http://www.bitcraze.se/. [08 2013].

[9] S. Fuller, A. Sands, A. Haggerty, M. Karpelson og R. Wood, «Estimating attitude and wind velocity using biomimetic sensors on a microrobotic bee,» *ICRA 2013.*

[10] C. Perry, «Robotic insects make first controlled flight,» Harvard SEAS Communications, [Internet]. Available: http://news.harvard.edu/gazette/story/2013/05/robotic-insects-make-first-controlled-flight/.

[11] H. Sato og e. all, «radio-controlled cyborg beetles: a radio-frequency system for insect neural flight control,» [Internet]. Available: http://www.eecs.berkeley.edu/~maharbiz/Sato_2009_WirelessFlightControl.pdf.

[12] M. Maharbiz, «Recent developments in the remote radio control of insect flight,» *Frontiers in NeuroscienceOther,* 2010.

[13] «Cyborg beetles to be the US military's latest weapon,» [Internet]. Available:

http://phys.org/news174812133.html. [11 2013].

[14] L. Petricca, C. Grinde og P. Ohlckers, «A miniaturized bulk micromachined triaxial accelerometer fabricated using deep reactive etching through a multilevel thickness membrane,» *ournal of Microsystem Technologies, Springer,* Vol. %1 av %2Volume 18, Number 5 , DOI: 10.1007/s00542-012-1429-9, pp. 613-622, 2012.

[15] L. Petricca og P. Ohlckers, «Analytic model and FEM characterization of two piezoresistive microphone membrane.,» *Advanced Materials Research,* nr. ISSN: 1022-6680, 2013.

[16] Sensonor, «Sensonor technologies,» [Internet]. Available: http://www.sensonor.com/%E5%85%AC%E5%8F%B8/technologies.aspx. [10 2013].

[17] D. Lampadau, «MultiMEMS Presentation,» Stimesi Course, 2009.

[18] SensoNor, «SA20,» [Internet]. Available: http://www.sm-elektronik.pl/pdf/SA20.pdf. [10 2013].

[19] SensoNor, «Products,» Sensonor, [Internet]. Available: http://www.sensonor.com/pressure-products/pressure-sensors.aspx.

[20] O. Elle, S. Halvorsen, M. Gulbrandsen, L. Aurdal, A. Bakken og Samset, «Early recognition of regional cardiac ischemia using a 3-axis accelerometer sensor.,» *Physiol Measure 26(4):429,* 2005.

[21] P. Halvorsen, A. Espinoza, L. Fleischer, O. Elle, L. Hoff, R. Lundblad og e. al, «Feasibility of a three-axis epicardial accelerometer in detecting myocardial ischemia in cardiac surgical patients,» *J Thoracic Cardiovasc Surg 136(6):1496–1502,* 2008.

[22] P. Halvorsen, L. Fleischer, A. Espinoza, O. Elle, L. Hoff, H. Skulstad og e. al, «Detection of myocardial ischaemia by epicardial accelerometers in the pig,» *Br J Anaesth 102(1):29–37.*

[23] C. Grinde, A. Sanginario, P. Ohlckers, G. Jensen og M. Mielnik, «Two clover-shaped piezoresistive silicon microphones for photo acoustic gas sensors,» *J. Micromech. Microeng.20,* Vol. %1 av %2doi:10.1088/0960-1317/20/4/045010, p. 11, (2010) 045010.

[24] L. Petricca, P. Ohlckers og G. Mellem, «Ultra low weight spacer for PCB2PCB interconnections,» *Journal of Microelectronics and Electronic Packaging, IMAPS,* vol. 1, nr. 1, 2014.

[25] hiconnex, «Axojump® Flat Flexible Cables (FFC),» [Internet]. Available: http://www.hiconnex.co.za/Axon_flat.html. [10 2013].

[26] 3M, «3754 Series,» [Internet]. Available: http://solutions.3m.com/wps/portal/3M/en_US/WW3/Country/?WT.mc_id=www.3M.com/us.

[27] L. Petricca, V. Hrishikeshavan, P. Ohlckers og I. Chopra, «Design, fabrication and test of an Embedded Lightweight Kinematic autopilot (ELKA),» *Submitted to International Journal of Intelligent Unmanned Systems,* nr. ISSN: 2049-6427, 2013.

[28] G. BOARD. [Internet]. Available: http://sourceforge.net/apps/mediawiki/warpwing/index.php?title=GINA2.2. [10 2013].

[29] ST microelectronics, «STM32F103,» [Internet]. Available: http://www.st.com/web/catalog/mmc/FM141/SC1169/SS1031/LN1565/PF189782. [8 2013].

[30] L. Petricca, P. Ohlckers og X. Chen, «The Future of Energy Storage Systems,» i *Energy Storage*, Intech, ISBN 979-953-307-768-9, 2013.

[31] Sedao, «wikipedia,» 2009. [Internet]. Available: http://en.wikipedia.org/wiki/File:Black_silicon_LP3.jpg.

APPENDIX

Publications

Article I

Micro- and Nano-Air Vehicles: State of the Art.
Luca Petricca, Ohlckers, Per and Grinde, Christopher: International Journal of Aerospace Engineering. Volume 2011, Article ID 214549, 17 pages.
DOI:10.1155/2011/214549

Papers not available in this file due to publisher's restrictions:

Article II

A miniaturized bulk micromachined triaxial accelerometer fabricated using deep reactive etching through a multilevel thickness membrane
Luca Petricca, Christopher Grinde and Per Ohlckers: Journal of Microsystem Technologies,
Springer, Volume 18, Number 5 (2012), 613-622, *DOI: 10.1007/s00542-012-1429-9*

Article III

Analytic model and FEM characterization of two piezoresistive microphone membrane
Luca Petricca; Per Ohlckers; MEMSM 2013: Proceedings of the MEMS Mechanics, 15-16 March
2013, Wuhan

Article IV

Ultra low weight spacer for PCB to PCB interconnections
Luca Petricca; Per Ohlckers; Geir M. Mellem, Accepted for publication in IMAPS Journal of Microelectronics and Electronic Packaging issue 1 January 2014
(ISSN 1551-4897)

Hindawi Publishing Corporation
International Journal of Aerospace Engineering
Volume 2011, Article ID 214549, 17 pages
doi:10.1155/2011/214549

Review Article

Micro- and Nano-Air Vehicles: State of the Art

Luca Petricca, Per Ohlckers, and Christopher Grinde

Department of Micro and Nano Systems Technology (IMST), Vestfold University College, P.O. Box 2243, 3103 Tønsberg, Norway

Correspondence should be addressed to Luca Petricca, luca.petricca@hive.no

Received 29 September 2010; Accepted 21 February 2011

Academic Editor: N. Ananthkrishnan

Micro- and nano air vehicles are defined as "extremely small and ultra-lightweight air vehicle systems" with a maximum wingspan length of 15 cm and a weight less than 20 grams. Here, we provide a review of the current state of the art and identify the challenges of design and fabrication. Different configurations are evaluated, such as fixed wings, rotary wings, and flapping wings. The main advantages and drawbacks for each typology are identified and discussed. Special attention is given to rotary-wing vehicles (helicopter concept); including a review of their main structures, such as the airframe, energy storage, controls, and communications systems. In addition, a review of relevant sensors is also included. Examples of existing and future systems are also included. Micro- and nano-vehicles with rotary wings and rechargeable batteries are dominating. The flight times of current systems are typically around 1 hour or less due to the limited energy storage capabilities of the used rechargeable batteries. Fuel cells and ultra capacitors are promising alternative energy supply technologies for the future. Technology improvements, mainly based on micro- and nanotechnologies, are expected to continue in an evolutionary way to improve the capabilities of future micro- and nano air vehicles, giving improved flight times and payload capabilities.

1. Introduction

Recently, a large number of studies on micro- and nano air vehicles (MAVs/NAVs) have been published [1–5]. MAVs are defined as small flying systems which are designed for performing useful operations [1]. In 1997, DARPA started a program called "MAV-project" where they presented some minimal requirements. In particular, they set the maximum dimension to be around 15 cm long, and the weight, including payload, to be less than 100 g [6]. Furthermore, flight duration should be 20 to 60 minutes. In addition to the MAV-project, DARPA started another program called nano air vehicles, which focus on the aim "to develop and demonstrate an extremely small (less than 15 cm), ultra-lightweight (less than 20 g) air vehicle system with the potential to perform indoor and outdoor military missions." [7].

In 2005, Pines and Bohorquez [8] published a review on the state of the art of unmanned air vehicles (UAVs), and many of the basic characteristics and challenges identified there are, to a large extent, valid also for NAVs, such as the challenges of maneuverability at low speed in confined spaces.

In [9], NAVs are defined as small air vehicles with an operating range less than 1 km, a maximum flight altitude around 100 m, endurance less than one hour, and maximum takeoff weight (MTOW) of 25 g while MAVs are defined as 5 kg MTOW with endurance around 1 hour and an operative range around 10 km.

In this paper, we will use the definition from [9] when referring to MAV and NAV. When referring to both classes of systems, the term AVS (air vehicle systems) will be used.

1.1. Research and Development of AVS. Many research institutions are actively studying and developing new air vehicles, reducing size and weight while improving performance, and adding more functionality. Examples here are Harvard Micro-robotics Laboratory in the USA [10], Department of Aeromechanics and Flying Engineering from Moscow Institute of Physics and Technology in Russia [4, 11], Aircraft Aerodynamics and Design Group at Stanford University (USA) [12, 13], the Autonomous Systems Laboratory at ETH Zurich (Switzerland) [14, 15], and Deptment of Precision Instrument and Mechanology at Tsinghua University in China [16]. Several companies and agencies also play an

important role in the manufacturing and development of AVS. Examples here are DARPA [7] from USA, Prox Dynamics [2, 17] from Norway, and Syma from USA.

1.2. Applications. AVS applications span a wide range, and the majority of them are military. AVS are capable to perform both indoor missions and outdoor missions in very challenging environments. The main applications are intelligence, surveillance, and reconnaissance (ISR) missions. These systems can provide a rapid overview in the area around the personnel, without exposing them to danger. Infrared (IR) cameras can give detailed images even in the darkness. Furthermore, NAVs, thanks to their reduced dimensions, are perfect for reconnaissance inside buildings, providing a very useful tactical advantage. As reported in [3], such small vehicles are currently the only way to remotely "look" inside buildings in the battlefield.

They can carry specific sensors such as gas, radiation or other sensors used to locate biological, nuclear, chemical, or other threats. They can, for instance, fly inside toxic clouds and transmit data or bring samples back to the base station, and, thus, provide vital information on the composition and extent of gaseous clouds and improve the assessment of danger.

Some of the applications described above can be extended to the civilian field. For example, the police and the fire brigade could use the capability of indoor flights for inspecting unsafe or collapsed buildings [2] in order to search for survivors or simply do a safety check of the building structure.

Since AVS would decrease the time necessary to explore a given area [3], they could be used in disaster cases, such as earthquakes, after hurricanes, or in collapsed mines [1]. In these cases, locating survivors faster increase the probability of saving lives.

However, AVS are not only related to high-risk applications, they can also be used as a support in regular police operations such as traffic control [1], crowd management or ordinary city surveillances.

Mass production of AVS will reduce the cost and, thus, enhance distribution among soldiers and policemen. This could render NAVs to be a natural part of the standard soldiers' equipment. In this case, one of the main features that NAVs must have is that they have to be ready for flight in a few seconds, without any lengthy startup procedures needed.

2. Challenges

AVS are not only scaled down versions of larger aircrafts "*they are affordable, fully functional, militarily capable, small flight vehicles in a class of their own*" [6]. With their reduced size, they have to keep all the features of larger aircraft in a small volume, which increase the complexity and challenges. However, in the last few years, the miniaturization progress of AVS has practically stopped [4] (See Figure 1). This mainly happened since there are several problems. There are both physical and technological challenges that slow down further miniaturization [4].

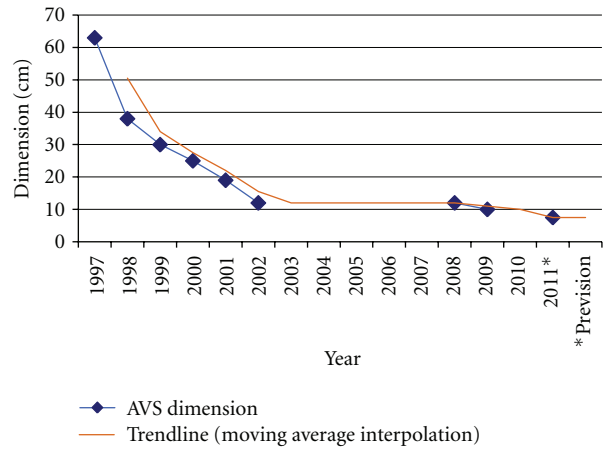

Figure 1: AVS development: dimension reduction; data from 1998–2002 [4] and 2008-2009 [2].

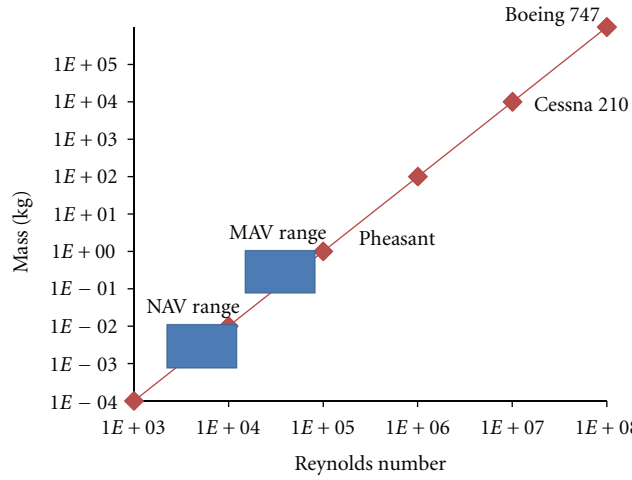

Figure 2: Reynolds number for aerial vehicles, adapted from [19].

The first problem that appears is related aerodynamics related to the low Reynolds number for AVS. This dimensionless number reflects the ratio between the inertial forces and the viscous forces and is defined [18] as

$$\text{Reynolds number} = \frac{\text{fluid density} \times \text{speed} \times \text{size}}{\text{viscosity}}. \quad (1)$$

For AVS, both speed and size are several orders of magnitude smaller than for large aircrafts. This gives Reynolds number, less than one-hundred thousand, which is less than one-tenth of what is common for a full-size aircraft (Figure 2). Flight in this aerodynamic domain is more difficult. Since other physical laws are governing in this domain, a lot of efforts have been made to understand ultralow Reynolds number flight, studying the flight of insects whose size is even smaller than NAV.

Although aerodynamics at low Reynolds numbers are not clearly understood yet [5], it is well know that for

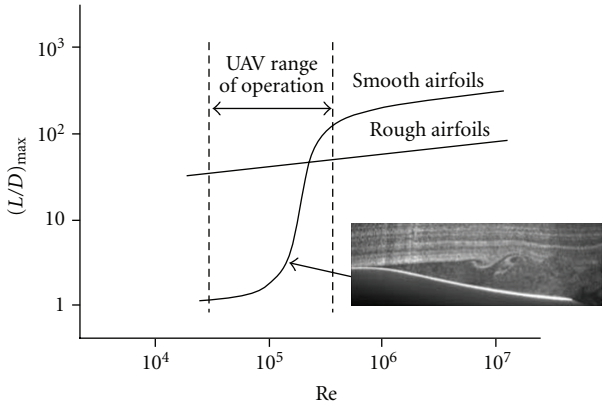

Figure 3: Lift-to-drag ratio variation with Reynolds number, reproduced from [73].

Reynolds numbers under 100,000, the aerodynamics efficiency (defined as lift-to-drag (L/D) ratio) rapidly decreases [19, 20] (Figure 3).

In addition to the physical challenges, given by the intrinsic reduction of physical parameters, there is also a problem of system integration. One can easily be misled to believe that larger aircrafts are much more complex than small AVS. The complexity of AVS becomes apparent if it is considered that they, similar to a larger aircraft, should be fully operational with respect to flight altitude, acceleration, stability, speed, and so forth, while the sensors and signal processing units, as illustrated in Figure 4, have to be integrated in a much smaller volume, with limited weight while keeping the power consumption to a minimum, increasing the challenges beyond that of larger aircrafts.

2.1. Weight Budget and Power Budget. During the design process of AVS, both the weight budget and the power budget should be carefully monitored. In particular, the total mass of the vehicle should be kept as low as possible, since added weight will increase power consumption. The minimum power required to keep a fixed-wing aircraft in level flight can be expressed as [13]

$$P = \frac{TV}{\eta_p} = \frac{W}{L/D}\frac{\left(2W/S\rho C_L\right)^{1/2}}{\eta_p}, \quad (2)$$

where T is the thrust, V is the velocity, η_p is the propeller efficiency, W is the weight, S is the wing area, ρ is density, and C_L is the lift coefficient. This means that doubling the weight nearly triples the power consumption. Similarly, for hovering flight, the power requirement is expressed as [13]

$$P = \frac{TV_h}{M} = \frac{W}{M}\left(\frac{W}{2S\rho}\right)^{1/2}, \quad (3)$$

where M is the figure of merit of the rotor and V_h is the induced velocity in hover. Similar to that described above, a doubling of the weight increases the power required by a factor of nearly 3.

An example weight budget for a 197 g MAV can be found in [15]. The details are presented in Figure 5.

A similar budget for a NAV can be found in [12], in which a 15 g vehicle is presented. However, a supercapacitor rather than a battery was used as a power source since no other technologies were able to "*satisfy the power requirement within the weight constraint*". Since the power density of supercapacitors at present is lower than that of batteries (see Section 5.3), the performance falls outside the specification for NAV. A more realistic comparison is, therefore, to replace the 5 g supercapacitor with a 6 g battery as used in [2, 12]. The modified weight budget for a 15 g AVS is, then, as illustrated in Figure 6.

It is interesting to see how the contributions from the various parts scale when the overall weight is reduced. A comparison of the information in Figures 5 and 6 after classifying the various parts in four categories (electronics, motors, battery, and airframe) can be found in Figure 7. It reveals that if the size is decreased, electronics still account for about 13% of the total weight, while motors, actuators and battery increase relatively. This reflects the difficulties of scaling down batteries and motors while maintaining acceptable performance.

When the system is miniaturized, the airframe has the greatest reduction in percentage. This is probably due to the ultralimited weight budget of the NAV that made the developer really optimize the airframe, carefully selecting shape and materials.

A similar comparison has been made for the power budget (Figure 8). It should be noted that, in this case, the MAV power budget has been adapted from [15] while for the NAV budget, we did not find any paper which explicitly reported such information, and for this reason, it was estimated. We used the theoretical estimate for a 15 g NAV found in [21]. For an additional margin to account for various system losses, the value was increased by ~15%, for instance, assuming an efficiency of the electric motor of 85% [22]. The required power was, therefore, increased from the reported 585 mW to 700 mW. With respect to the communication systems, the authors in [16] report an example of a handmade RF communication apparatus that weighs 8 g, which we assume could be adapted to be used in an NAV. The power consumption of this transmitter is reported to be around 500 mW. For the remaining onboard devices, among them a camera [23], the power requirement was estimated to be about 50 mW. Comparing the corresponding power budgets, as seen in Figure 8, we find that by downscaling the weight, the NAV at less than one-tenth of the weight of the MAV, relatively uses less power to generate lift. Since the power consumption of the communication system is dependent on factors like distance, bit rate, data compressions, and so forth, rather than size, the relative requirement in the NAV is significantly higher.

3. AVS Typologies

AVS can be classified into four main typologies depending on their method of propulsion and lift. These are fixed wings,

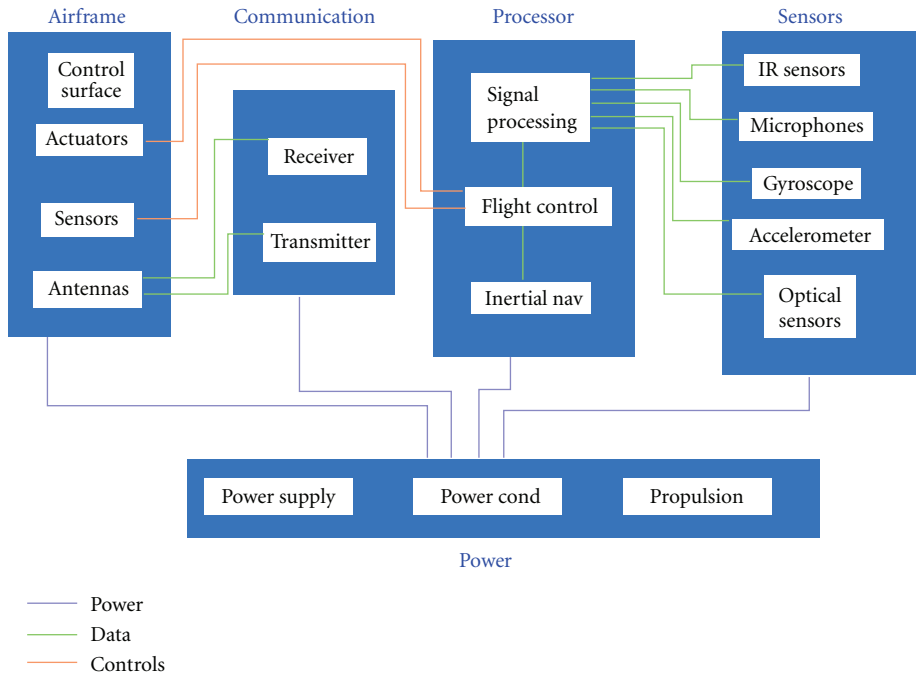

Figure 4: AVS system integration, adapted from [6].

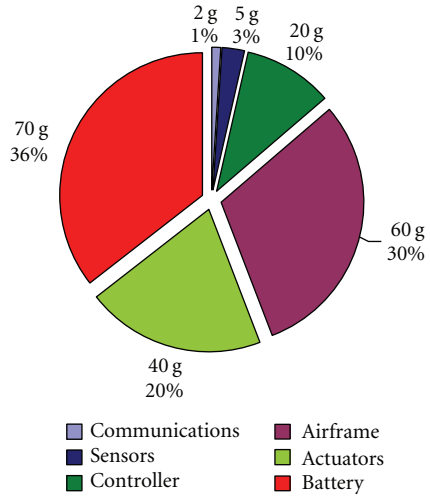

Figure 5: Weight budget for 197 g AVS as presented in [15].

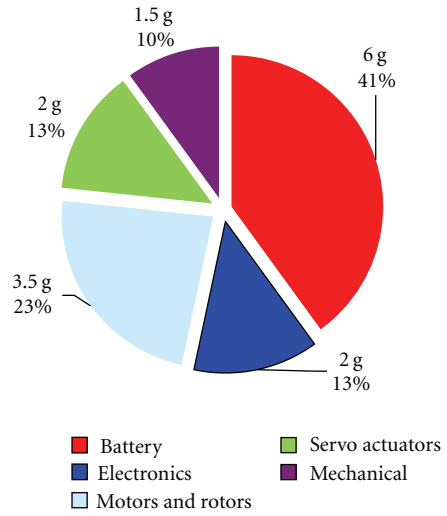

Figure 6: AVS weight budget allocation: the first number is the weight in grams while the second one is the percentage with respect to the total weight of 15 g, adapted from [2, 12].

rotary wings, and flapping wings. The fourth class is without propulsion and is called passive.

In the followings sections, we will briefly review one or more examples from each class, and analyze their main advantages and disadvantages.

3.1. Fixed Wings. Among the different typologies of AVS, fixed wing is the most developed and the easiest to design and build, because "*well-established design methods for larger operational fixed-wing UAV could be applied with some precautions and modified aerodynamic characteristics*" [20]. Several prototypes have already *been proposed to customers* [1]. These kinds of vehicles require relative high speed for flight, typically 6 to 20 m/s. As they are incapable to hover or fly any slower, indoor flight is very challenging and is often avoided. Examples of suitable applications are location of forest fires, searching for people at sea, and missions where low speed is not required.

Fixed-wing aircrafts require a thrust-to-weight ratio less than 1, since wings provide an additional lift [13]. The full

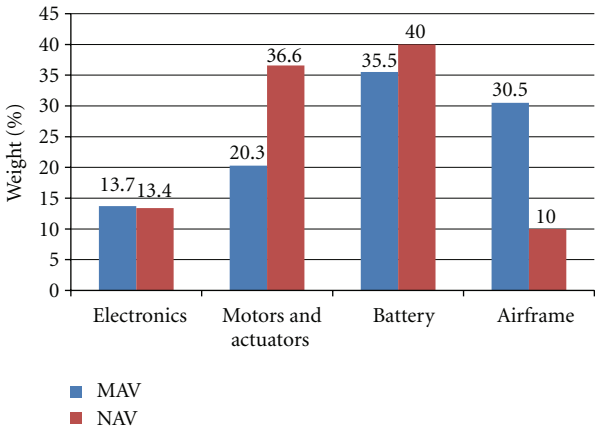

Figure 7: AVS weight budget allocation in percentage with respect to the total weigh calculated for a 197 g MAV and 15 g NAV.

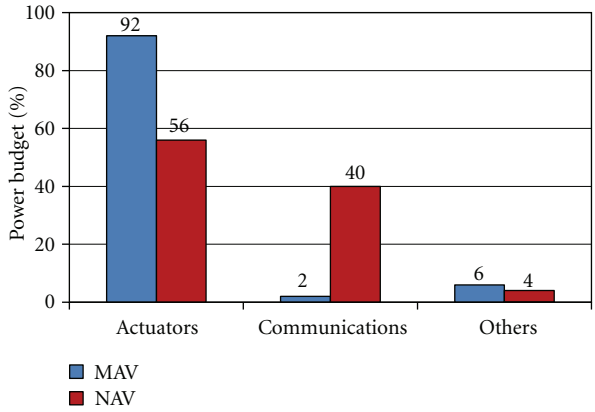

Figure 8: AVS power budget allocation in percentage calculated for a 197 g MAV and 15 g NAV.

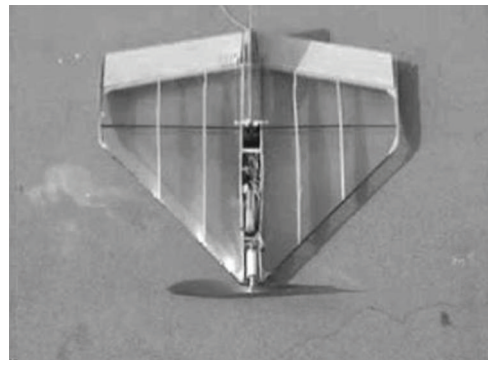

Figure 9: TH360 prototype MAV [16].

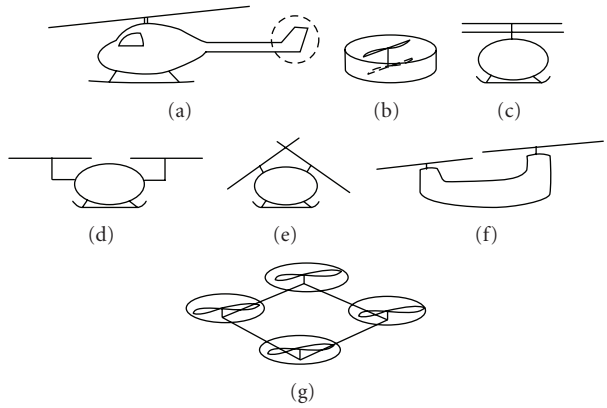

Figure 10: Graphic representation of rotary-wing configurations: (a) conventional configuration, (b) ducted coaxial, (c) conventional coaxial, (d) rotors side by side, (e) synchropter, (f) conventional tandem, (g) quad rotor [27].

Table 1: Performance summary for the first-generation Black Widow MAV [24].

Total mass	56.5 g
Loiter drag	9.4 g
Lift/drag ratio	6.0
Loiter velocity	11.2 m/s
Loiter lift coefficient	0.42
Loiter throttle setting	70%
Endurance	33.4 min

weight is divided by the L/D ratio, and, thus, they require less power to fly than a helicopter with the same weight hovering, where the weight is completely balanced by the propulsion thrust [13]. This efficiency gain is most obvious in larger aircrafts where the L/D ratio reaches values of more than 30. Unfortunately, as we explained in the Section 2, this parameter rapidly decreases as the dimensions and correspondingly, the Reynolds number decrease (Figure 3). For this reason, the obvious advantage of a large aircraft becomes less pronounced when the ratio L/D is reduced to less than 10.

Several prototypes exist, but none are in the NAV range [9]; the existing AVS models have wingspans larger than 15 cm and thus are considered MAVs. In [16], two examples of fixed-wing MAVs are shown. One of these, the TH360 (Figure 9) includes a color video camera that transmits realtime images to the control station. The propulsion is from an electric motor, the wingspan is 45 cm and the total weight is around 120 g.

The main drawback of the system is the limited 5-minute flight endurance. Another fixed-wing MAV, often referred to, is the black widow [24] which was developed in 2001 by AeroVironment Inc. in collaboration with DARPA. The performance of this MAV is reported in Table 1.

Notice that the flight endurance is much longer than for the TH360 in [16] discussed above. The L/D ratio is only 6 for this 15 cm wingspan MAV, which is less than one-fifth of typical commercial airliners.

Rigid wings were used in all of the examples presented above. In contrast, in [25], a flexible-wing MAV is reported and compared with a rigid thin-wing MAV of the same size and shape. The motivation for this comparison is

"*for highlighting the distinct aerodynamic advantages of the flexible wing*." The conclusion is that a "*deformable wing is expected to harvest an intrinsic benefit: a portion of the energy that would normally be lost to the wing-tip vortices and wake, downstream of the MAV, now is stored as elastic strain energy in the wing's structure*" [25]. Following from this, it is found that flexible wings provide better *L/D* ratio than rigid wings for angles of attack ($\acute{\alpha}$) smaller than 10°.

3.2. Rotary Wings. The second type of MAV typology are systems with rotary wings. These AVS basically have the same structure as macroscale helicopters and, thus, are able to fly at quite high speeds, hover, and execute vertical take-off and landing (VTOL). These features make them perfect for indoor flight and short-range reconnaissance. Due to larger power requirement for hovering and VTOL, the endurance is also the bottleneck for this kind of AVS. With the miniaturization, a lot of challenges arise. Examples are low efficiency of the rotor system and the low thrust-to-weigh ratio [26]. Despite these disadvantages, rotary AVS are the only configuration capable to "*combine acceptable high and low speed characteristic including hovering*" [1]. Furthermore, they are also "*the only controllably hovering object at the moment*" [1].

Based on the number and position of the propellers, there are several possible configurations for rotary AVS. In Figure 10, some of the possible configurations are reproduced from [27].

Each one of these configurations has some specific features that make them suitable for specific types of missions.

Table 2 reports various aspects of the six typologies. Choice of configuration will depend upon the mission requirements. For example, if one wants to build AVS that are easy to maneuver, one should focus more on quad-rotor configuration and discard coaxial, but if we need AVS with low structural complexity, then quad-rotors are not the optimal choice anymore.

In general, when a designer needs to choose the best configuration, he will use a combination between these different selection criteria. In [27, 28], a weight parameter is assigned to each selection criteria to identify which feature is more important.

Several prototypes of these configurations are reported in the literature. In 2004, Epson built a prototype of small ducted coaxial AVS [29].

This "flying robot" had a wingspan of 136 mm and a total weight, including batteries, of 12.3 g. At 3 min, the endurance was the weak point of this prototype.

AVS with an improved flight time of 10 minutes are described in [30]. However, compared to the AVS in [29], the AVS in [30] had a total weight around 110 g and only one rotor, and, in this case, the torque is balanced by changing the angles of the yaw control surfaces [30], so these two systems are not directly comparable.

The T-REX model, provided by ALIGN Corporation [31], is a good example of a conventional configuration rotary MAV. It is an electrical powered AVS with rotor diameter less than 50 cm and a total weight around 340 g.

Table 2: Selection criteria of different rotary AVS typologies [27] (1: bad, 10: very good).

Selection criteria	Conventional (a)	Ducted coaxial (b)	Coaxial (c)
Compactness of folding	1	2	10
Reliability	9	10	8
Controllability	5	5	7
Aerodynamic cleanliness	8	2	8
Maturity of technology	10	8	10
Hover efficiency	10	8	8
Aerodynamic interaction	7	7	7
Vibration	1	2	1
Cruise efficiency	7	6	8
Maneuverability	5	3	3
Ease of payload packaging	10	8	10
Simplicity of structure	8	8	10
Simplicity of control system	6	6	6
Selection criteria	Side by side (d)	Tandem (f)	Quad-rotor (g)
Compactness of folding	2	2	8
Reliability	8	8	9
Controllability	5	5	10
Aerodynamic cleanliness	6	6	2
Maturity of technology	9	10	5
Hover efficiency	10	10	8
Aerodynamic interaction	10	10	7
Vibration	2	2	2
Cruise efficiency	6	6	5
Maneuverability	4	4	9
Ease of payload packaging	10	10	8
Simplicity of structure	8	8	7
Simplicity of control system	6	6	10

Despite that this configuration is the most common for larger aircrafts, it suffers from the disadvantage that it is difficult to control with respect to the quad-rotors configuration. For this reason, a lot of research has recently been put into the control of AVS with quad-rotors. A basic study on control theory presented in [32] shows how quad-rotor AVS could easily be controlled by changing the rotation speeds of the motors. The same principle is used in [12, 14]

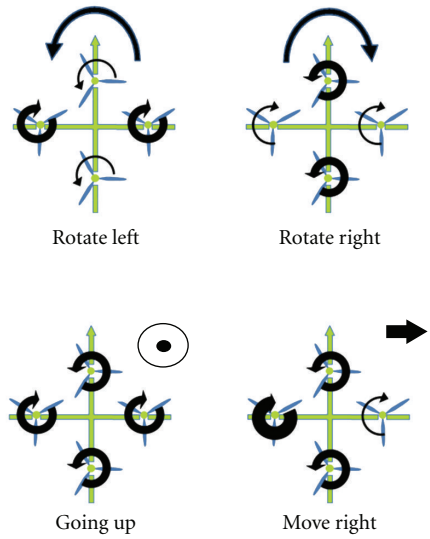

Figure 11: Quad-rotor concept motion description, the arrow width is proportional to propeller rotational speed adapted from [14].

and is illustrated in Figure 11. The torque is cancelled by making two rotors rotating clockwise and two rotors rotating counterclockwise. Despite the simple control systems and the ease of maneuverability of the quad-rotor systems, there are two main disadvantages that could limit their success. In particular, quad rotors mean four motors that are very power consuming [14]. Furthermore, motors are, in general, heavy and difficult to miniaturize. For these reasons this configuration should be avoided when the main target is to maximize flying time.

3.3. Flapping Wings. Both fixed wings and rotary wings provide mature and well-know technologies, but have problems due to the high unsteady effects due to reduction of Reynolds numbers. This motivated researchers to investigate alternative typologies. The basic idea was adapted from nature and uses the same flying technique as insects and birds: flapping wings. Since this idea came up, a lot of studies have been done in order to investigate the efficiency of such methods and the possibility to reproduce them in the laboratory. In fact, the principal motivation seems to be the possibility to "*integrate lift and thrust together with stability and control mechanism*" [33]. However, when we refer to this class of vehicles, we should make a distinction between bird-like vehicles called ornithopters and insect-like vehicles called entomopters. These two subclasses of flapping wings have completely different features. Ornithopters, like the majority of birds, generate lift by flapping wings up and down with synchronized small variations of angle of incidence. This method of thrust generation require forward flight similar to fixed-wing AVS [1]. As a result, ornithopters cannot hover, and they need to obtain an initial airspeed before taking off [1]. Entomopters use the kinematics of insects for flying, meaning a "*large and rapid change of angle of incidence*" [1]. Due to this large angle variation between the upstroke and downstroke, this technique is sometimes also referred to as pitch reversal. Compared to how birds fly, they are able to generate much more lift and, thus, are able to execute VTOL [1] and hovering.

With these two advantages, entomopters are much more interesting to adapt to AVS than ornithopters, and therefore we will mainly discuss Entomopters. Insects generate wing beats by contraction of muscles. The muscles can either generate wing motion through direct attachment or through indirect attachment, where the wing motion is generated, for example, through deforming the shape of the thorax [34, 35] (Figure 12). Large insects with lower beat frequency use both these modes of flying while smaller insect use mainly indirect muscles [35].

Linear actuators are the most suitable means for reproducing this motion. However, none of the available actuators match natural "*muscles over all the main performance characteristics*" [35]. The most promising technology is electroactive polymers (EAP) that is able of providing high energy density and high efficiency. In [36, 37], the possibility of using EAPs to reproduce artificial muscles is investigated. Even though it looks very promising, this technology is still under development and thus not yet widely available in commercial actuators.

A possible concept is to develop a flapping-wings mechanism using rotary actuators such as electric motors. In [34, 35, 38], three different methods for translating rotary motion into flapping-wings motion are presented (one example is shown in Figure 13). All three uses a crank rocker technique, but differ with respect to how they generate the pitch motion of the wing.

Despite this, a recent study [39] has shown that it is also possible to generate stable forward flight using simple motion without any feedback control of the wing movement.

Another important aspect of flapping air vehicles is the shape of the wings. In the literature, many different designs are reported; however, most of them try to reproduce bird or insects wings.

One distinction can be made between smooth wings and rough wings. Several test runs by the authors of [39] show that creating rough wings helps to increase the performance, since they "*are needed to prevent feathering deformation and produce a large up-down body motion*" [39].

Regarding wings, they are in general fabricated using micromachined molds. The molded wings are in general made from polymers like thermoset resins [39, 40].

3.4. Other Techniques. While the three typologies described above are the most common, some authors have started to investigate alternative techniques that could be useful in some cases. The most important class are the passive AVS. In [10, 41], a "palm-sized autonomous glider" (Figure 14) with a 10 cm wingspan weighing only 2 g is described. Since this class of vehicles does not have generation of thrust, meaning they are passive, they need to be hand launched or dropped, for example, from aircrafts.

Another example of an alternative topology is a blimp or airship. Although an unmanned airship is presented in [42],

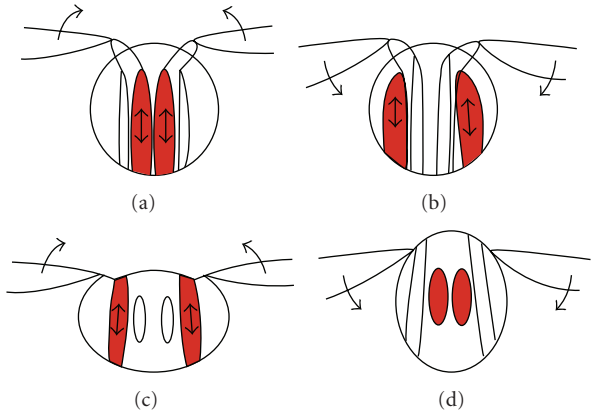

Figure 12: Insect wings beat generation: direct muscles (a, b) and indirect muscles (c, d) [35].

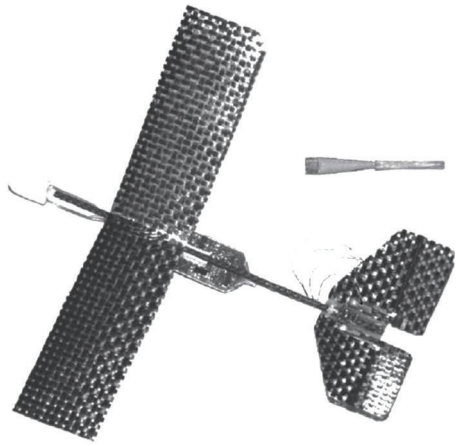

Figure 14: Palm-size micro glider [41].

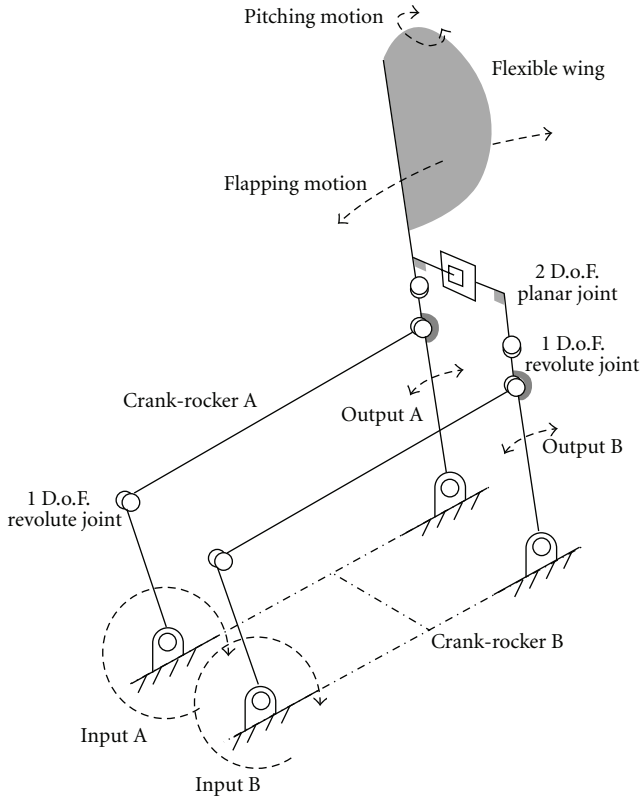

Figure 13: Rigid-body representation of the parallel crank-rocker mechanism. Full revolutions at inputs A and B produce reciprocating outputs A and B, which cause the wing to flap. Introducing a phase lag between the two linkages (and hence outputs) introduces a pitching motion to the wing [35].

the dimensions are out range of the specification of NAV and MAV.

4. AVS Typologies Comparison

Among the different typologies presented, it is important to choose one that offers the greatest advantages in terms of reliability, efficiency, and suitability for the application areas presented in Section 2. Unfortunately, none of these typologies have advantages only, and thus compromises must be made. Since fixed-wing vehicles are able to fly with much less thrust with respect to their real weight, they are perfect for relative large area control and high autonomy missions. Unfortunately, as we reported in Figure 3, the L/D ratio sharply decreases as soon as the Reynolds number decreases below 500000, and, thus, the main advantages of this typology (low consumption) become less pronounced compared to larger aircrafts. Since the Reynolds number decreases rapidly with miniaturization, the obvious advantages of the fixed-wing topology compared to other typologies such as helicopters, becomes less pronounced.

Also, since fixed wing topologies are incapable of hovering, they are less suitable for finding and overseeing targets. In [43], an algorithm that allows fixed-wing vehicles to lock on to the target while flying is investigated. The results are still unsatisfactory and too complex. In addition, their lack of hovering capabilities also renders them less suitable for indoor missions. For many customers, such as military and tactical squads, this limitation is not acceptable.

For users that require hovering capability, rotary-wing typology appears to be a good solution. In addition to hovering, they offer good maneuverability and medium complexity.

This is also the only configuration capable to "*combine high and low speed characteristics* [1].

The main disadvantage of rotary wings is the relative high power consumption. To overcome this problem, many researchers have investigated flapping wings. The basic idea is that if insects have this kind of propulsion, and they are able to generate high lift, they are probably very energy efficient. Unfortunately, this is challenging, since nature and engineering are based on different evolution processes. Nowadays, it is still not fully documented whether this method provides better efficiency than the much simpler rotary wing principle [13]. Some authors [38, 44] claim that they provide better performances, others [11] claim the contrary. However, these studies are not very comprehensive and should be considered

Table 3: Flying principle comparison focused on ability to miniaturization [14] (1: bad, 2: medium, 3: good).

	Fixed	Rotary	Bird	Blimp
Power cost	2	1	1	3
Control cost	2	1	1	3
Payload	3	2	2	1
Maneuverability	2	3	3	1
DOF	1	3	3	1
Stationary fly	1	3	2	3
Low-speed fly	1	3	2	3
Vulnerability	2	2	3	2
VTOL	1	3	2	3
Endurance	2	1	2	3
Miniaturization	2	3	3	2
Indoor usage	1	3	2	2
Total	*20*	*28*	*26*	*26*

with caution. In [21], a comparison between a flapping-wing system and a rotary-wing system is done. It is reported that the hover efficiencies only differ with less than 5% and thus are almost negligible. Therefore, it can be assumed that both principles have comparable efficiency in the ultralow Reynolds number regime. However, rotary-wing systems are simpler and can, therefore, more easily be miniaturized. In addition, "*they are also the only controllably hovering flying objects at the moment*" [1].

For this reason, rotary wings are acknowledged as the most suitable topology for NAV [11, 13, 21]. Table 3 shows one comparison table reproduced from [14].

5. Rotary Wings: Main Part Analysis

In this section, conventional helicopter NAVs are reported and analyzed. Many of the discussions made in this section can be easily extended to the other typologies, since technologies such as energy storage, propulsion, and communications, are independent of the typology.

5.1. Airframe. It is well known in aerodynamics that the shape that provides the best aerodynamic performance in subsonic speed is the drop-based shape [45].

The design begins typically with finding placements for large components such as motors and battery. During this step, the center of gravity of the system and its location should also be considered. This space optimization is not an easy problem. In [46], an example of design optimization and positioning of the center of mass for a nano-helicopter is presented. In particular, a generic-based algorithm is used for "*organizing a given set of components and payloads such that the resulting flight vehicle has the most compact overall size and still fulfills the given physical and control constraints*" [46]. Once all the parts of the system have been allocated, it is possible to start to design the enclosures of the vehicle as a double drop-shaped hull (Figure 15).

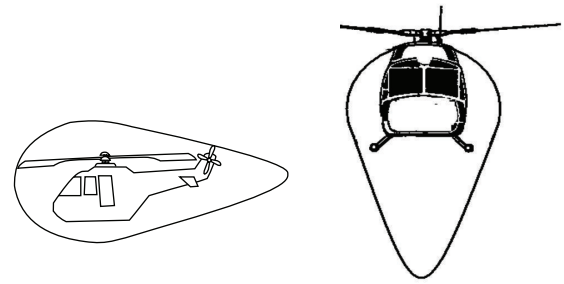

Figure 15: Double drop section: lateral view (left) and vertical section (right).

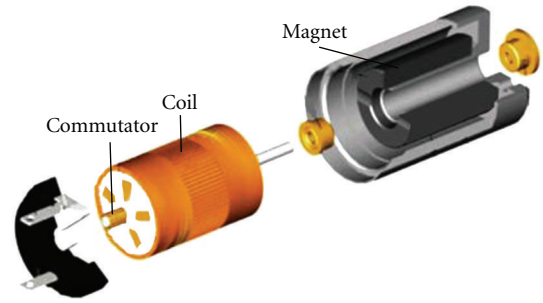

Figure 16: Coreless motor structure, from [74].

The horizontal drop shape (Figure 15(left)) is needed to reduce the aerodynamic drag during forward flight. Since the main rotor pushes down the air, it will create an airflow that pushes the helicopter body towards the ground, increasing the power consumption. Once more, a drop-shape body cross-section (Figure 15(right)) will reduce the drag forces, reducing the power consumption further. Airframe design can truly be considered much more than an aesthetic endeavor. Due to the lack of useful simulators in the ultralow Reynolds number regime, many companies base their development more on workmanship experience than on simulations.

Carbon fiber composites are the main materials used for AVS airframes, because they have high strength-versus-weight ratio and are easily accessible.

5.2. Propulsion. All the three active AVS typologies presented above need to generate motion. There are several ways to make an air vehicle fly. The most common and easiest way is to use electric motors. Almost all the existing prototypes use electric motors due to their high efficiencies, reliability, and ease of control.

Since coreless motors are lighter and smaller than, for example, direct current (DC) iron-core motors, they are considered more suitable. As their name indicates, there is no iron core inside their motor structure. The magnet is positioned directly inside the coil, and then the rotor coil is wrapped around the magnets without using any iron material as illustrated in Figure 16.

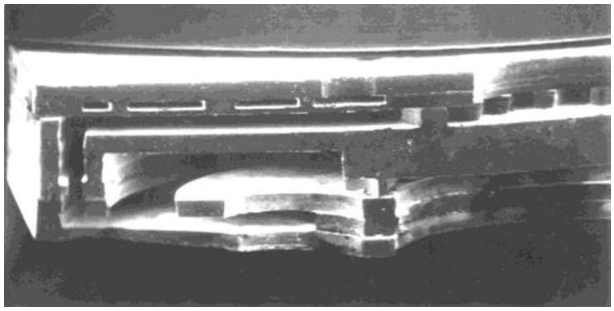

Figure 17: Micro gas turbine, SEM image [49].

In addition to the small dimensions and the low weight, another advantage of coreless motors is the lack of iron losses that are reflected in a higher efficiency. Furthermore, since the rotor is very light, it has a small inertia that allows extremely fast accelerations and decelerations.

However, the lack of iron in the center reduces the motor heat dissipation. To avoid overheating and thermal problems, they are only used for small and low-power motors.

Although an electric motor is the most suitable for AVS applications, it can be seen in Figure 8 that more than the half of the electric energy present in the AVS is used to generate lift. It could, therefore, be advantageous to replace electric motors with other systems, such as gas turbine or internal combustion engines (ICE). Two AVS examples using ICE are presented in [47], in which a motor provided by Cox Company were used. However, as the engine of this vehicle was quite large, it will be difficult to integrate into future NAVs. Most recent studies on miniaturized ICE [48] show that, with the current technology, it is possible to build a miniaturized combustion motor of 0.3-0.4 cc.

Even though ICE motors are interesting for AVS applications; they suffer of one big disadvantage compared to electric motors: they are very noisy. This limits the application in NAVs that have to be used for tactical missions, where it is required to have high stealth skills.

Micro-gas turbines could be another alternative. In [49], an example of the fabrication of an extremely small turbine with dimensions around 2 cm × 2 cm × 0.4 cm with a combustion chamber of 0.195 cubic cm is given. It has been built using six silicon wafers and configured for hydrogen fuel (Figure 17).

ONERA Company announced in 2008 that they had demonstrated a micro gas turbine suitable for AVS. Their turbine can supply from 50 to 100 W with dimensions around 2-3 cm for the diameter and the height [50]. The combustible in this case could be either hydrogen or propane (Figure 18).

Despite significant efforts by numerous groups [49, 51], no known commercialization of MEMS gas turbine generators are currently known.

Finally, the possibility to include a hybrid system, such as electric motors and combustion engines should be mentioned. Although this technique has been already used with good results in larger air vehicles [52], it is not suitable for smaller systems such as NAV in which both weight and size represent very strict constraints.

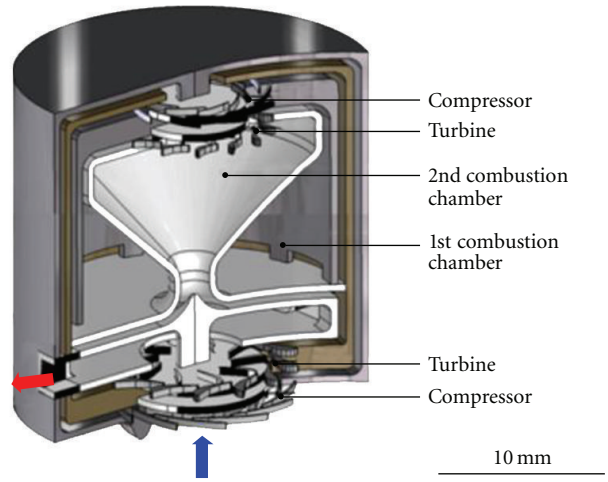

Figure 18: Architecture of the ONERA Micro gas turbine, reproduced from [50] ONERA, the French Aerospace Lab.

5.3. Energy Storage. All the active AVS typologies need electric energy on board to feed the electronic circuits, sensors, actuators, and the communication devices. Furthermore, if electric motors are used, a large part of the electric energy will be used for the propulsion supply motors. Since energy stored in batteries does not require any conversion to be useful for both the electronics and propulsion, batteries seem to be the most appropriate for electric MAV. Furthermore, the energy density of the batteries has steadily increased during the last years, mainly thanks to the effort of the companies producing smart phones, notebooks, and other consumer electronics. In 2006, the battery market reached 50 billion dollars and is expected to expand to more than 70 billion in 2011 [53]. As a result, many companies continue to invest large amounts of money on battery research, mainly focusing on reducing dimensions and increasing the energy density.

Ni-Cd batteries have now almost completely been replaced by more energy dense lithium-based batteries that also are less toxic [53]. Furthermore, the most advanced batteries (intelligent batteries) include circuitry that optimizes the cells' discharge curves with respect to the loads. They "*exploit various battery-related characteristics such as charge recovery effect, to enhance battery lifetime and ensure safe operation*" [54].

Unfortunately, despite these improvements, the most advanced batteries also provide much lower energy densities than sources, such as gasoline or methanol, as shown in Figure 19.

Methanol could be used in a gas turbine as presented in the previous section, providing much more power compared to battery based systems.

Another alternative is fuel cells. A fuel cell system is conceptually a sort of battery in which the fuel is transformed into electric current trough an electrochemical process. There are several kinds of fuel cells which mainly differ with respect to the principle of energy conversion. Currently, the most promising fuel cells for AVS are proton exchange membrane (PEM) fuel cell and direct methanol fuel cell

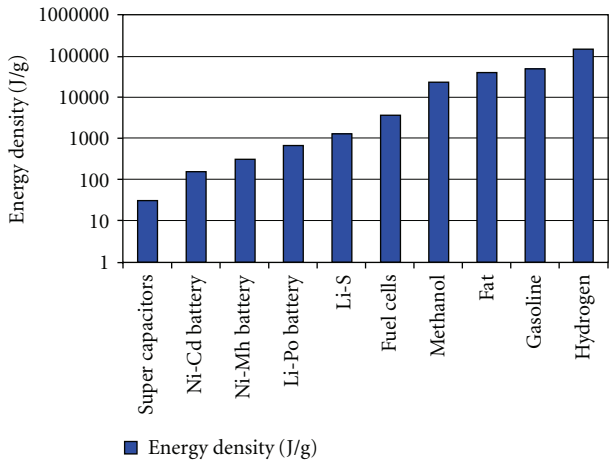

Figure 19: Energy densities of various energy storage systems, graph adapted from [33, 53, 75–77].

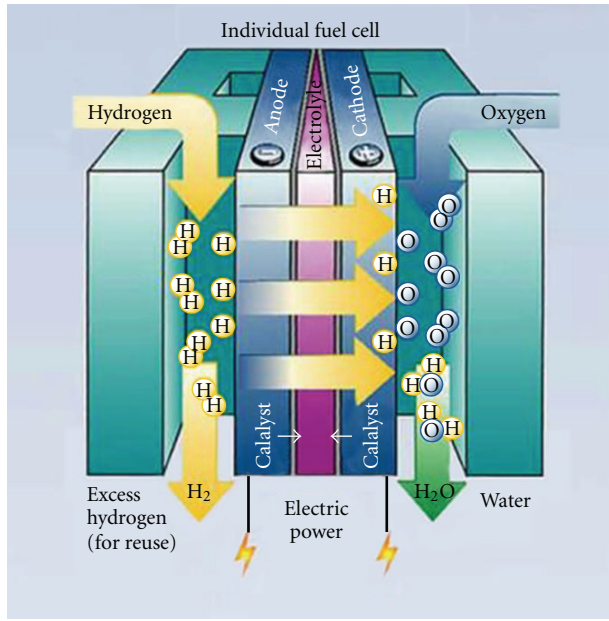

Figure 20: PEM fuel cell principle [78].

(DMFC) which could be considered as a subcategory of the PEM.

The schematic of a PEM fuel cell is reported in Figure 20 [51]. It basically consists of an anode catalyst and a cathode catalyst separated by a membrane that can be crossed only by protons. In the classical configuration, PEM uses hydrogen on the anode side and oxygen on the cathode side.

The hydrogen atoms that reach the anode catalyst dissociate into protons and electrons. The protons can cross through the membrane and reach the cathode. Here they will react with oxygen to form water. The electrons left behind the membrane are forced to "travel" inside the electric circuit, generating an electric current. It is clear that, in this case, the only residual waste is water, and thus this is very environmental friendly. Unfortunately, hydrogen does not occur naturally and thus has to be produced by chemical processes, wasting energy. Furthermore, hydrogen has a high mass energy density (143000 J/g) but a very low volumetric energy density (10790 J/L), which makes it difficult to store. In fact, it has to be transformed to liquid form, compressed at high pressure, or transformed to other forms with high volumetric densities, such as metal hydride.

To overcome this problem, several new kinds of cells have been developed. Among these, one of the most interesting is the DMFC. It uses pure methanol as fuel, which simplifies the fuel storage.

The working principle is similar to PEM, but the chemical reactions are a little bit more complicated. DMFC residual wastes are water and carbon dioxide, and the overall cell efficiency is lower compared to a PEM cell.

These fuel cells are already available in the market [55], with quite small dimensions (several cm) and low weight (few hundred grams). An example of an MAV powered by a fuel cell is "The Hornet", developed in 2003 by DARPA, it "*uses absolutely no batteries, capacitors, or other sources of energy*" (except fuel cells) [56]. The Hornet has a wingspan of 38 cm and a total weight of the vehicle around 170 g, including fuel.

Since the weight budget of NAVs is very limited, further development is required before fuel cells become a viable alternative energy source.

Besides fuel cells, ultracapacitors have become interesting the last few years. The latest improvements have made this power storage principle attractive also for AVS applications, and they have already been used in some prototypes [12]. Since they are an evolution of normal capacitors, their main features are fast charging, high peak current, and virtually unlimited charge-discharge cycles [57]. The main drawback consists of the output voltage that strongly depends on the charge status of the capacitor. *By the time an ultracapacitor reaches a 25-percent state of charge, its voltage has dropped by half* [57]. Besides this, when compared with other energy sources, they have a relative low energy density. Recently, in [58], a new electrostatic nanocapacitor (shown in Figure 21) which "*dramatically increases energy storage density of such devices—by a factor of 10 over that of commercially available devices—without sacrificing the high power they traditionally characteristically offer*" was announced.

Ultracapacitors are, therefore, candidates to play an important role for future energy storage systems in AVS. Solar cells should also be mentioned as a potential useful energy source. Even though photovoltaic systems are interesting for AVS, the small dimensions of NAVs, the weight budget constraints, and the mainly indoor application area (low light) limit the efficiency and the available energy.

5.4. Transmissions. Basically, for AVS, two different kinds of signals have to be transmitted: control signals and data signals. The control signals are needed for take-off, landing and for piloting the vehicle in general while the data signals are basically the data collected by onboard sensors of AVS, such

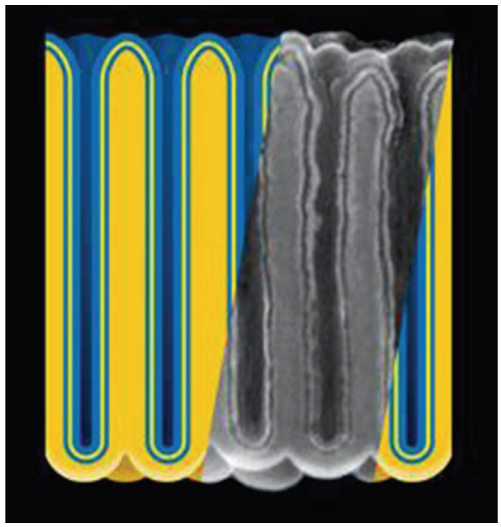

Figure 21: Electrostatic nanocapacitor. Developed by Maryland NanoCenter [58].

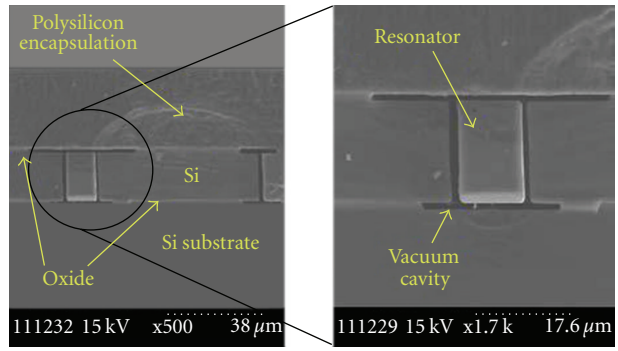

Figure 22: Example of an MEMS resonator [59].

as camera, microphones, gas sensors, and so forth, which for many applications need to be transmitted to a base station.

Control signals are mainly transmitted from the ground station to the vehicle while the data is sent from the vehicle to the user. An example of control communication systems on board is given in [16], where they developed a home-made RF transmitter for use onboard an MAV. With a weight of 8 g, it could transmit at 56 mW. The transmitter operated at a frequency range between 1.18 and 1.45 GHz. Furthermore, a microdemodulator operating at 50 MHz and weighing 5.4 g was used at the receiver end [16].

Another example is found in [25], where only a receiver was used onboard. In particular, the receiver, including a phase locked loop (PLL), weighed around 12 g, and it consisted of a 7-channel pulse code modulation system. Since no data was to be sent back to the base station no transmitter was required on board that vehicle.

When reducing the AVS dimensions, the major challenges for the communications parts are represented by the weight and size of the antennas, filters, and resonators. Antenna shape strongly depends on the operating frequencies and, thus, will depend on external factors, such as application (military frequencies are different from civilian frequencies), distances, bit rate, and so forth. This requires the antenna design to be application specific.

The size, weight, and performance of resonators depend on the operating frequency. Several examples of micromechanical resonators for various frequency ranges can be found in the literature. In Figure 22 is shown one example of it reproduced from [59]. Since quartz resonators suffer from high power consumption and relative bulky size [59], developing MEMS resonators could help overcome these drawback, and, thus, this is the most interesting candidate for substituting the quartz resonators [60].

Other examples of filters and resonators can be found in [61, 62], where systems for 22 GHz and 140 MHz bands were described.

Such devices can help to not only decrease the overall power consumption of the communications systems, but their small size and weight relative to the quartz systems they replace also help reduce the size, weight and power consumption of the overall system.

5.5. Sensor and Actuators. Sensors can roughly be divided into two categories. The first one contains the sensors that are necessary for flight control, the second is sensors that are a part of the payload and provide mission-specific information.

Theoretically, AVS should be able to fly only with a 3-D accelerometer and a 3-D gyroscope. Ideally, if we know the initial position, we will be able to calculate all the later positions only by integrating the resulting vector acceleration two times to find the position, while 3-D gyroscope signal is used to maintain flight stability. However, since all gyroscopes and accelerometers suffer from offsets and drifts, for instance with time and temperature, the accuracy of the calculated position will decrease over time. Additional sensors can be used to compensate somewhat for drifts and offsets. For example, in [63], it is stated that "*accelerometers and gyros can only be used for the pitch and the roll, while for yaw measurements, magnetometers have to be used*" [63]. In fact, if the roll rate is integrated with respect to time to find the roll angle, it "*will lead to drifting errors*" [63]. Another interesting solution is presented by the "Paparazzi project" described in [64], in which "*a free and open-source hardware and software project intended to create an exceptionally powerful and versatile autopilot system*" is described. The proposed solution uses two infrared (IR) sensors positioned on the side walls of the AVS.

The basic concept is that if the vehicle is perfect parallel to the earth surface, then both the sensors will detect the same temperature and thus get the same signal. On the other hand, if there is any misalignment (Figure 23), one sensor will reveal the earth temperature (warmer) while the other one will reveal the sky temperature (colder). Based on this principle, it is possible to correct for the tilt angle. Furthermore, it is also feasible to use more than one pair, for calculating not only the roll angle but also the pitch angle. However, even though this method is very useful for larger AVS, it has poor functionality for NAVs, especially

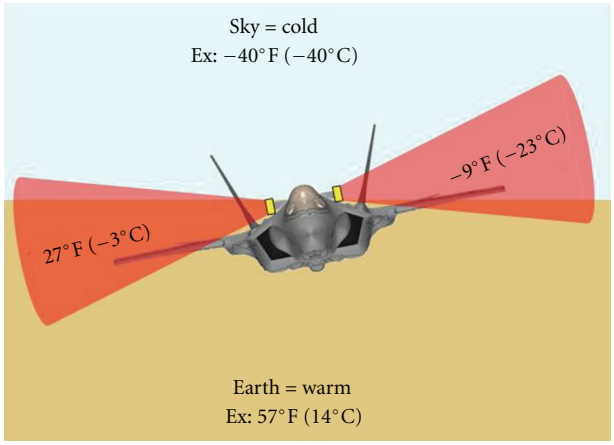

Figure 23: Example of angle compensation using two IR sensors reproduced from [64] under GNU FDL 1.2.

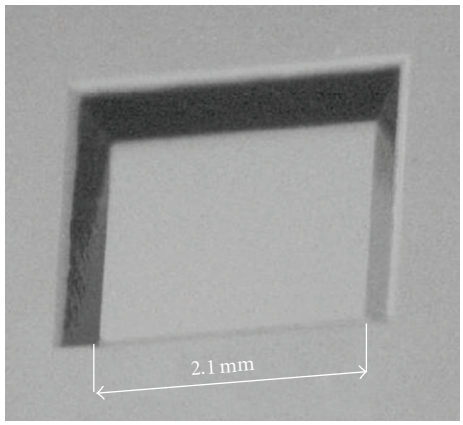

Figure 24: Example of ultrasmall microphone, diaphragm [66].

during indoor missions where this kind of IR tracking works poorly because the IR radiation signals are more or less unpredictable.

For NAV applications, in which each extra sensor means additive space, power, and weight, the system should be kept as simple as possible, using for example very low drift gyroscopes or accelerometers or using some compensation circuitry.

The other class of sensors is the data-collecting sensors that provide useful information for the users. Examples are cameras, microphones, gas sensors, biological sensors, radiation sensors, and so forth. Depending on the applications, most AVS will include one or more of these data sensors.

Cameras and microphones are two of the most useful data sensors for AVS. A camera is required to help the user pilot the vehicles when there is no direct vision between them (e.g., in indoor missions). Similarly as for batteries, smart phones and other consumer electronics have driven the development. The smallest available cameras nowadays are based on CMOS sensors which offer "*advantages in on-chip functionality, system power reduction, low cost and miniaturization*" [65] when compared with the earlier used CCD image sensors.

Figure 25: Graphic representation of the GCS from Prox Dynamics, containing three NAVs in the bottom side while the controls and the LED screen are placed on the upper side [17].

Microphones are useful in spying, rescue operations, and similar applications. Today, micro- and nanotechnologies allow building very small microphones, such as those in [66] with diaphragm dimension of $2.1 \times 2.1\ \text{mm}^2$ (Figure 24) using a "*single-crystalline wafer as the substrate for the microphone capsule*" [66].

Micro- and nanotechnologies also provide great improvements for gas sensors, since "*the sensitivity of chemical gas sensors is strongly affected by the specific surface of sensing*" [67]. Using nanotechnologies, it is possible to build nano structures with a larger sensing area and either keeping the sensitivity constant while reducing the size or increasing the sensitivity while keeping the size constant. Many different materials can be used for building gas sensors. Some examples can be found in [68] where metal oxide is used, or in [69] that presents gas sensors based on conducting polymers. Depending on the application, a range of other sensors can also be used. In this case, important selection criteria for the choice of sensor are small dimensions, low weight, and low power consumption.

Actuators are needed for different applications on board AVS. They are used for flight control, for instance, making the vehicle turn, for moving the sensors, for example, movable cameras or for building useful tools, such as micropliers for picking up samples. Similarly as for flapping-wing systems, linear actuators are theoretically the most suitable solution for this application. Although there are a lot of studies of new materials and new concepts for linear actuators, all the existing prototypes have limited maximum elongation and/or long response time that limit the applicability on board AVS. The suboptimal solution is using microservo actuators that are rotary actuators. They consist of a small electric motor, with some cogwheels that form a microgear. In 2002, a microharmonic drive was realized as one of the smallest microbacklash-free servo actuator in the world [70] with a size of 6 mm in diameter (another version is available with 8 mm diameter size) and

Table 4: Quality comparison of actuators: adapted from [35, 79].

Actuators	Advantages	Disadvantages
Linear actuators		
Piezoelectric Ceramic	(i) Excellent performances except strain output (ii) Strain output can be magnified using bender arrangements	(i) Require high activation voltage
Shape memory alloy	(i) Excellent performance except frequency range	(i) Poor fatigue life
Magnetostrictor	(i) Excellent performances except strain output	(i) Require high activation voltage
Solenoid	(i) High strain	(i) Low energy density
Electroactive Polymers (EAP)	(i) Dielectric elastomers outperform muscle in both stress and strain output.	(i) Only ionic EAPs operate on low voltage (ii) Novel technology not widely available
Rotary actuators		
Electric motors	(i) Efficiency (ii) Reliability (iii) Versatility	(i) Weight (ii) Dimensions

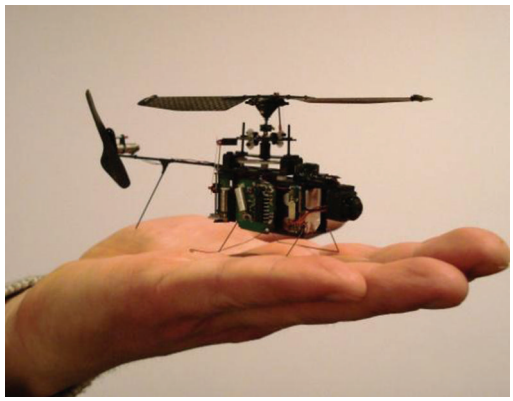

Figure 26: The Hornet 2-b (Prox Dynamics), complete with camera and video transmitter [17].

with only 1 mm axial length. It is made with nickel-iron, and it has an output torque of 50 mNm (for the 8 mm diameter gear). Other rotary actuator technologies, such as piezoelectric motors [71] or shape alloy motors [72], are still under development, and they are yet not mature enough for AVS applications. Table 4 shows a quality comparison of some linear and rotary actuators.

6. Future Trends

Considering the short-term future (1–3 years from mid-2010), rotary-wing NAV will be the most important commercial type, since it has the best performing technology at present and the near future. Prox Dynamics [17] has prototypes that will be available on the market in 2011. They present a system consisting of two parts: the NAV and the ground control station (GCS). The GCS (shown in Figure 25) has three different uses: (1) tt will protect the vehicles during the transport, (2) it will be used as remote control system for the NAV in flight. (3) As a station for recharging the AVS batteries. The whole system (NAV + GCS) will have a total weight less than 1 kg, and dimensions of 15 cm × 15 cm × 5 cm [2] (Figure 26).

These systems will be customizable by the clients and equipped with different sensors depending on mission needs.

Specifications for those AVS state that will be able to fly for up to 30 minutes with a 10 m/s maximum speed. It has a video camera and transmitter for the video signal to the GCS.

However, in the future, flapping-wing solutions are viable and will improve maneuverability and efficiency relative to rotary NAVs. Several technologies can potentially replace batteries as power supplies in future NAV. Recent advances make ultracapacitors a good candidate. However, depending on future developments, fuel cells are also promising, in particular direct methanol fuel cells, where the fuel storage is less complicated than for hydrogen-based fuel cells.

Further size and weight reductions of communication systems are important issues for the future. Micro- and nanoelectromechanical systems (MNEMS) technologies can be used to provide devices, such as lighter, smaller, and less power consuming resonators and filters than the current state of-the-art devices. However, reducing antenna dimensions while keeping acceptable performance is challenging since antenna performance is related to size governed by the laws of electromagnetic radiation. Furthermore, the transmission power cannot be reduced under a certain threshold without degrading the quality of the communication. MNEMS actuators will also replace the relative heavy rotary actuators (based on small electric motors), with lighter and more energy efficient linear actuators based on new materials, such as electroactive polymers. However, the improvements will be relatively small, since the avionics on board of an NAV are already ultraminiaturized (a few grams).

Future NAVs will most likely be equipped with GPS and radar systems. Infrared and/or high-definition cameras could be included. Mission-specific sensors and actuators could be removed and replaced depending on the application. A quick-connection method can help to, for example, rapidly replace a gas sensor with a radiation sensor in a few seconds. Nanotechnology could play an important role also

in aerodynamic improvements. For instance, a combination of different thin deposited layers of functional materials could allow the realization of morphable wings. These wings will be able to change their shape in accordance with the flying regime in order to maximize, in realtime, the efficiency of the vehicle. The shape changing can for example be on the attach angle or on the wing surface roughness.

Future trends could also include the development of sophisticated software that will enable operating future ultrasmall NAVs in coordinated swarms. Furthermore, with the future improvements of artificial intelligence, some of them will have decision-making capabilities, opening the way to completely new mission profiles.

7. Conclusions

In this article, the main typologies of air vehicle systems used for micro- and nano-air vehicles have been presented. The typologies are fixed-wing, rotary-wing, flapping-wing and passive AVS. For each type, the main features are described, with a particular focus on their advantages and disadvantages. Several examples of existing prototypes have been described, and a final comparison between fixed-wing, rotary-wing, flapping-wing, and passive AVS have been presented. The rotary-wing principle is at present, and in the near future, in most NAV applications, the best option since they are capable to hover and have good maneuverability in NAV range dimensions. Military surveillance and reconnaissance are the most promising applications for such vehicles. Flapping-wing typology adapted from nature, first of all entomopters adapted from insects, is a promising future option, but more long-term research is needed to make this typology practical for AVS in general and for NAVs.

Power requirements and power sources for NAVS are major challenges for present and future NAVs, resulting in limited flight times around or less than 30 minutes and payload capabilities around 10 grams or less. Rechargeable batteries, mostly rechargeable lithium ion batteries will in the near future, remain the main power source in NAVs, with most of the power used by the electric motors. Fuel cells and ultracapacitors show promising potentials to be used in the future, but more research and development are needed to make them practical and with high enough power density for use in NAVs. In addition, the development of a new class of gas turbines, which have already been proven promising, can surprise us in the near future. Sensors will play an increasingly important role, as they will be more and more used for improving flight control and collecting various information data from the environment during missions. For special missions and requirements, new sensor classes have to be developed; they will be focused on having low weight and low power consumption. Communications will remain a challenge as the power consumption scales poorly with size reduction of the NAVs. Micro- and nanotechnologies are enabling technologies for NAVs that will evolutionarily contribute to further size and weight reductions, improved sensors and actuators for better flight control and data collection during missions, and improved energy sources with higher power densities.

Acknowledgments

This work is performed as part of a contract research for Prox Dynamics in the "Mosquito" project, supported by the Norwegian Research Council. Trygve Fredrik Marton and Geir Morten Mellem from Prox Dynamics are acknowledged for their support and suggestions for this paper.

References

[1] C. Galiński and R. Zbikowski, "Some problems of micro air vehicles development," *Bulletin of the Polish Academy of Sciences: Technical Sciences*, vol. 55, no. 1, pp. 91–98, 2007.

[2] D. H. Paulsen, "Nano UAS- an upcoming reality," in *Proceedings of the 24th International Unmanned Air Vehicles Conference*, Bristol, UK, 2009.

[3] R. J. Bachmann, "Biologically inspired mechanisms facilitating multi modal locomotion for areal micro-robot," in *Proceedings of the 24th International Unmanned Air Vehicles Conference*, Bristol, UK, 2009.

[4] S. V. Serokhvostov, "Ways and technologies required for MAV miniaturization," in *Proceedings of the European Micro Air Vehicle Conference (EMAV '08)*, Braunschweig, Germany, July 2008.

[5] W. Shyy, Y. Lian, J. Tang et al., "Computational aerodynamics of low Reynolds number plunging, pitching and flexible wings for MAV applications," *Acta Mechanica Sinica*, vol. 24, no. 4, pp. 351–373, 2008.

[6] M. James and C. M. S. F. McMichael, "Micro Air Vehicles—Toward a New Dimension in Flight," 1997, http://www.fas.org/irp/program/collect/docs/mav_auvsi.htm.

[7] T. Hylton, "Nano Air Vehicle program," 2010, http://www.darpa.mil/dso/thrusts/materials/multfunmat/nav/index.htm.

[8] D. J. Pines and F. Bohorquez, "Challenges facing future micro-air-vehicle development," *Journal of Aircraft*, vol. 43, no. 2, pp. 290–305, 2006.

[9] U. Yearbook, *UAS: The Global Perspective*, vol. 164, UAS Yearbook, 7th edition, 2009/2010.

[10] R. J. Wood, S. Avadhanula, E. Steltz et al., "An autonomous palm-sized gliding micro air vehicle—design, fabrication, and results of a fully integrated centimeter-scale MAV," *IEEE Robotics and Automation Magazine*, vol. 14, no. 2, pp. 82–91, 2007.

[11] S. V. Serokhvostov, "Flapping wings efficiency investigation on the basis of physical law conservation," in *Proceedings of the European Micro Air Vehicle Conference (EMAV '08)*, Braunschweig, Germany, 2008.

[12] I. Kro, F. Prinz, and M. Shantz, "A miniature rotorcraft concept phase II final report," Tech. Rep., Stanford University, Palo Alto, Calif, USA, 2001.

[13] I. Kroo and P. Kunz, "Development of the mesicopter a miniature autonomous rotorcraft," in *Proceedings of the American Helicopter Society Vertical Lift Aircraft Design Conference*, American Helicopter Society, San Francisco, Calif, USA, 2000.

[14] S. Bouabdallah, P. Murrieri, and R. Siegwart, "Towards autonomous indoor micro VTOL," *Autonomous Robots*, vol. 18, no. 2, pp. 171–183, 2005.

[15] S. Bouabdallah, M. Becker, and R. Siegwart, "Autonomous miniature flying robots: coming soon!," *IEEE Robotics and Automation Magazine*, vol. 14, no. 3, pp. 88–98, 2007.

[16] H. Wu, D. Sun, and Z. Zhou, "Micro air vehicle: configuration, analysis, fabrication, and test," *IEEE/ASME Transactions on Mechatronics*, vol. 9, no. 1, pp. 108–117, 2004.

[17] Prox Dynamics, http://www.proxdynamics.com.

[18] J. Happel and H. Brenner, *Low Reynolds Number Hydrodynamics: With Special Applications to Particulate* , Springer, New York, NY, USA, 1983.

[19] T. J. Mueller, "Aerodynamic measurements at low raynolds numbers for fixed wing micro-air vehicles," Tech. Rep., University of Notre Dame, Notre Dame, The Netherlands, 2000.

[20] I. M. A.-Q. A. A. M. Al-Bahi, "Micro aerial vehicles design challenges: state of the art review," in *Proceedings of the SAS UAV Scientific Meeting & Exhibition*, Jeddah, Saudi Arabia, 2006.

[21] Z. L. A. J.-M. Moschetta, "Rotary vs. flapping-wing nano air vehicles: comparing performances," in *Proceedings of the European Micro Air Vehicle Conference (EMAV '09)*, Delft, The Netherlands, 2009.

[22] M. Wing and J. F. Gieras, "Calculation of the steady state performance for small commutator permanent magnet DC motors: classical and finite element approaches," *IEEE Transactions on Magnetics*, vol. 28, no. 5, pp. 2067–2071, 1992.

[23] P. Ferrat, C. Gimkiewicz, S. Neukom, Y. Zha, A. Brenzikofer, and . Thomas Baechler, "Ultra-miniature omni-directional camera for an autonomous flying micro-robot," in *Optical and Digital Image Processing*, Proceedings of SPIE, April 2008.

[24] J. M. Grasmeyer, "Development of the black widow micro air vehicle," in *Proceedings of the 39th AIAA Aerospace Sciences Meeting and Exhibit*, M. T. Keennon, Ed., American Institute of Aeronautics and Astronautics, 2000.

[25] F. Zhang, R. Zhu, P. Liu, W. Xiong, X. Liu, and Z. Zhou, "A novel Micro Air Vehicle with flexible wing integrated with on-board electronic devices," in *Proceedings of the IEEE International Conference on Robotics, Automation and Mechatronics (RAM '08)*, pp. 252–257, September 2008.

[26] D. Schafroth, S. Bouabdallah, C. Bermes, and R. Siegwart, "From the test benches to the first prototype of the muFly micro helicopter," *Journal of Intelligent and Robotic Systems*, vol. 54, no. 1–3, pp. 245–260, 2009.

[27] A. Datta, "The martian autonomous rotary-wing vehicle (MARV)," Tech. Rep., University of Maryland, College Park, Md, USA, 2000.

[28] A. Datta, B. Roget, D. Griffiths et al., "Design of a Martian autonomous rotary-wing vehicle," *Journal of Aircraft*, vol. 40, no. 3, pp. 461–472, 2003.

[29] World's Lightest Micro-Flying Robot Built by Epson, Available from: http://www.physorg.com/pdf860.pdf.

[30] G. B. Kim, "Design and performance test of rotary wing micro air vehicle without tail rotor," in *Proceedings of the European Micro Air Vehicle Conference (EMAV '08)*, Braunschweig, Germany, July 2008.

[31] Corporation, "A. T-Rex 250," http://www.align.com.tw/html.

[32] J. Kim, M. S. Kang, and S. Park, "Accurate modeling and robust hovering control for a quad-rotor VTOL aircraft," *Journal of Intelligent and Robotic Systems*, vol. 57, no. 1–4, pp. 9–26, 2010.

[33] G. R. Spedding and P. B. S. Lissaman, "Technical aspects of microscale flight systems," *Journal of Avian Biology*, vol. 29, no. 4, pp. 458–468, 1998.

[34] R. Madangopal, Z. A. Khan, and S. K. Agrawal, "Energetics-based design of small flapping-wing micro air vehicles," *IEEE/ASME Transactions on Mechatronics*, vol. 11, no. 4, pp. 433–438, 2006.

[35] A. Conn, S. Burgess, R. Hyde, and C. S. Ling, "From natural flyers to the mechanical realization of a flapping wing micro air vehicle," in *Proceedings of the IEEE International Conference on Robotics and Biomimetics (ROBIO '06)*, pp. 439–444, December 2006.

[36] P. Brochu and Q. Pei, "Advances in dielectric elastomers for actuators and artificial muscles," *Macromolecular Rapid Communications*, vol. 31, no. 1, pp. 10–36, 2010.

[37] Y. Fujihara, T. Hanamoto, and F. Dai, "Fundamental research on polymer material as artificial muscle," *Artificial Life and Robotics*, vol. 12, no. 1-2, pp. 232–235, 2008.

[38] M. A. A. Fenelon and T. Furukawa, "Design of an active flapping wing mechanism and a micro aerial vehicle using a rotary actuator," *Mechanism and Machine Theory*, vol. 45, no. 2, pp. 137–146, 2010.

[39] H. Tanaka and I. Shimoyama, "Forward flight of swallowtail butterfly with simple flapping motion," *Bioinspiration and Biomimetics*, vol. 5, no. 2, Article ID 026003, 2010.

[40] H. Tanaka and R. J. Wood, "Fabrication of corrugated artificial insect wings using laser micromachined molds," *Journal of Micromechanics and Microengineering*, vol. 20, no. 7, Article ID 075008, 2010.

[41] R. J. Wood, S. Avadhanula, E. Steltz et al., "Design, fabrication and initial results of a 2g autonomous glider," in *Proceedings of the 31st Annual Conference of IEEE Industrial Electronics Society (IECON '05)*, pp. 1870–1877, November 2005.

[42] J. Kuhle, *An Airship for Cooperative Robot Tasks*, IFAC, Portugal, 2003.

[43] J. Saunders and R. Beard, "Tracking a target in wind using a micro air vehicle with a fixed angle camera," in *Proceedings of the American Control Conference (ACC '08)*, pp. 3863–3868, June 2008.

[44] U. Pesavento and Z. J. Wang, "Flapping wing flight can save aerodynamic power compared to steady flight," *Physical Review Letters*, vol. 103, no. 11, Article ID 118102, 2009.

[45] M. Cavendish, *Growing Up with Science*, Marshall Cavendish, Tarrytown, NY, USA, 3rd edition, 2006.

[46] T. T. H. Ng and G. S. B. Leng, "Design optimization of rotary-wing micro air vehicles," *Proceedings of the Institution of Mechanical Engineers, Part C: Journal of Mechanical Engineering Science*, vol. 220, no. 6, pp. 865–873, 2006.

[47] S. J. Morris, "Design and flight test results for micro-sized fixed-wing and VTOL aircraft," in *Proceedings of the International Conference on Emerging Technologies and Factory Automation*, 1997.

[48] I. Sher, D. Levinzon-Sher, and E. Sher, "Miniaturization limitations of HCCI internal combustion engines," *Applied Thermal Engineering*, vol. 29, no. 2-3, pp. 400–411, 2009.

[49] A. Mehra, X. Zhang, A. A. Ayon, I. A. Waitz, M. A. Schmidt, and C. M. Spadaccini, "Six-wafer combustion system for a silicon micro gas turbine engine," *Journal of Microelectromechanical Systems*, vol. 9, no. 4, pp. 517–527, 2000.

[50] Onera company, http://www.onera.fr/defa/micro-machines-thermiques-mems.

[51] X. C. Shan, Z. F. Wang, R. Maeda, Y. F. Sun, M. Wu, and J. S. Hua, "A silicon-based micro gas turbine engine for power generation," in *Proceedings of the Symposium on Design, Test, Integration and Packaging of MEMS/MOEMS (DTIP '06)*, Stresa, Italy, April 2006.

[52] R. R. Glassock et al., "Multimodal hybrid powerplant for unmanned aerial systems (UAS) robotics," in *Proceedings of the 24th Bristol International Unmanned Air Vehicle Systems Conference*, University of Bristol, Bristol, UK, 2009.

[53] D. C. Müller, *Energy Storage: Strong Momentum in High-End Batteries*, Credit Suisse, Suisse, 2007.

[54] S. K. Mandal, P. S. Bhojwani, S. P. Mohanty, and R. N. Mahapatra, "IntellBatt: towards smarter battery design,"

in *Proceedings of the 45th Design Automation Conference (DAC '08)*, pp. 872–877, June 2008.
[55] FuelCellStore, http://www.fuelcellstore.com.
[56] DARPA, "Micro air vehicle powered entirely by fuel cell makes debut flight," in News, April 2003.
[57] IEEE Spectrum, "Circuit Could Swap Ultracapacitors for Batteries," June 2001, http://spectrum.ieee.org/semiconductors/design/circuit-could-swap-ultracapacitors-for-batteries.
[58] Maryland, U.o. 2010, http://www.nanocenter.umd.edu/news/news_story.php?id=3773.
[59] B. Kim, R. N. Candler, M. Hopcroft, M. Agarwal, W. T. Park, and T. W. Kenny, "Frequency stability of wafer-scale encapsulated MEMS resonators," in *Proceedings of the13th International Conference on Solid-State Sensors and Actuators and Microsystems (TRANSDUCERS '05)*, pp. 1965–1968, Stanford University, June 2005.
[60] Discera, "Mems based oscillators," http://www.discera.com.
[61] K. M. Strohm, F. J. Schmückle, B. Schauwecker, J. F. Luy, and W. Heinrich, "Silicon micromachined RF MEMS resonators," in *Proceedings of the IEEE MSS-S International Microwave Symposium Digest*, pp. 1209–1212, June 2002.
[62] S. A. Bhave, DI. Gao, R. Maboudian, and R. T. Howe, "Fully-differential poly-SiC lamé-mode resonator and checkerboard filter," in *Proceedings of the 18th IEEE International Conference on Micro Electro Mechanical Systems (MEMS '05)*, pp. 223–226, February 2005.
[63] M. Palaniappan et al., "Unmanned Vehicle Group Semester Report," Tech. Rep., Purdue University Aeronautics and Astronautics, 2010.
[64] The Paparazzi Project, http://paparazzi.enac.fr/wiki/Main_Page.
[65] L. Q. Wang, Y. Shi, Z. Lu, and H. Duan, "Miniaturized CMOS imaging module with real-time DSP technology for endoscope and laryngoscope applications," *Journal of Signal Processing Systems*, vol. 54, no. 1–3, pp. 7–13, 2009.
[66] T. Tajima, T. Nishiguchi, S. Chiba et al., "High-performance ultra-small single crystalline silicon microphone of an integrated structure," *Microelectronic Engineering*, vol. 67-68, pp. 508–519, 2003.
[67] B. Ding, M. Wang, J. Yu, and G. Sun, "Gas sensors based on electrospun nanofibers," *Sensors*, vol. 9, no. 3, pp. 1609–1624, 2009.
[68] S. Palzer, E. Moretton, F. H. Ramirez, A. Romano-Rodriguez, and J. Wöllenstein, "Nano- and microsized metal oxide thin film gas sensors," *Microsystem Technologies*, vol. 14, no. 4-5, pp. 645–651, 2008.
[69] H. Bai and G. Shi, "Gas sensors based on conducting polymers," *Sensors*, vol. 7, no. 3, pp. 267–307, 2007.
[70] MicroHarmonicDeviceGroup, "Hollow shaft micro servo actuators realized with the Micro Harmonic Drive," 2002, http://www.mikroharmonicdrive.de.
[71] J. Liu, Z. Yang, H. Zhao, and G. Cheng, "Novel precision piezoelectric step rotary actuator," *Frontiers of Mechanical Engineering in China*, vol. 2, no. 3, pp. 356–360, 2007.
[72] I. Spinella, G. Scirè Mammano, and E. Dragoni, "Conceptual design and simulation of a compact shape memory actuator for rotary motion," *Journal of Materials Engineering and Performance*, vol. 18, no. 5-6, pp. 638–648, 2009.
[73] A. Santhana and K. J. D. Jacob, "Effect of regular surface perturbations on flow over an airfoil," in *Proceedings of the 35th Fluid Dynamics Conference*, American Institute of Aeronautics and Astronautics, Toronto, Canada, 2005.
[74] CITIZEN MICRO CO., LTD., 2009, http://www.citizen-micro.com/tec/corelessmotor.html.
[75] M. Bronz et al., "Towards a long endurance MAV," *International Journal of Micro Air Vehicles*, vol. 1, no. 4, pp. 241–254, 2009.
[76] G. Elert, http://hypertextbook.com/facts/2005/MichelleFung.shtml.
[77] Technologies, M., http://www.maxwell.com.
[78] Institute, G.E.N, "Fuel cell," http://www.geni.org/globalenergy/library/technical-articles/generation/title-page-images/fuelcell.jpg.
[79] C. Tetrault, http://www.rctoys.com/rc-products-catalog/RC-AIRPLANES.html.